

# UMEÅ UNIVERSITY MEDICAL DISSERTATIONS

New series No 801-ISSN 0346-6612 ISBN 91-7305-269-8

---

From the

Department of Radiation Sciences, Umeå University, Sweden,  
Department of Biomedical Engineering and Informatics,  
Umeå University Hospital, Sweden, and  
Department of Applied Physics and Electronics,  
Umeå University, Sweden

## **Resonator sensor technique for medical use**

**An intraocular pressure measurement system**

by

**Anders Eklund**



Umeå University

2002

© Anders Eklund 2002

ISBN 91-7305-269-8

Printed by Grafiska enheten,  
Västerbottens Läns Landsting,  
Umeå, Sweden, 2001

*”Mistakes are the friends of success.  
Deny them and they become the enemy.”*  
**Dartwill Aquila**

To Maria, Anton and Sanna



## Abstract

In the work of this doctoral dissertation a new resonator sensor technique, first presented in 1989, has been further developed and evaluated with focus on technical characteristics and applications within the medical field.

In a first part a catheter-type tactile sensor using the resonator sensor technique was evaluated in a silicone model and applied to human prostate *in vitro*. The main finding was that different histological compositions of prostate tissue correlated with the frequency shift,  $\Delta f_s$ , of the resonator sensor and that the common property was the hardness of the tissue. The results indicated that hardness of the prostate tissue, and maybe hardness of human tissue in general, can be expressed according to a cone penetration standard (DIN ISO 2137) and that the hardness can be measured with this tactile sensor system. The tissue hardness application for the resonator sensor technique has to be further developed and evaluated in a larger study. The study also produced results that has led to the basic understanding of the resonator sensor system. One important result was that  $\Delta f_s$  of the sensor system was related to the contact area between sensor and sample. This indicated that the resonance sensor could be used for contact area measurement.

In a second part, containing three studies, the area-sensing capability from the first study was utilised in the development and evaluation of the applanation resonator sensor (ARS) for measurement of intraocular pressure (IOP). For the purpose of evaluating IOP-tonometers, an *in vitro* pig-eye model was developed, and it was shown that a saline column connected to the vitreous chamber could be used successfully to induce variations in IOP.

A ARS sensor with a flat contact surface was applied onto the cornea with constant force and  $\Delta f_s$  was measured. A mathematical model based on the Imbert-Fick law and the assumption that  $\Delta f_s$  was linearly related to contact area was proposed and verified with a convincing result. IOP measured with the ARS correlated well ( $r=0.92$ ,  $n=360$ ) with the IOP elicited by a saline column.

The ARS in a constant-force arrangement was evaluated on healthy human subjects *in vivo*. The results verified the sensor principle but revealed a non-negligible source of error in off-centre positioning between the sensor and cornea. The sensor probe was redesigned and evaluated in the *in vitro* model. The new probe, with a spherical contact surface against the eye reduced the sensitivity to off-centre positioning. It was also shown that a  $\Delta f_s$  normalisation procedure could reduce the between-eye differences.

The ARS method for IOP measurement was further developed using combined continuous force and area measurement during the dynamic phase when the sensor initially contacts the cornea. A force sensor was included with the resonator sensor in one probe. Evaluation was performed with the *in vitro* pig-eye model. The hypothesis was that the IOP could be deduced from the differential change of force and area during that phase. The study showed good accuracy and good reproducibility with a correlation of  $r=0.994$  ( $n=414$ ) between measured pressure in the vitreous chamber and IOP according to the ARS. Measurement time was short, 77 ms after initial contact. Problems with inter-eye differences and low resolution at high pressures were reduced. The ARS method is the first to combine simultaneous, continuous sampling of both parameters included in the applanation principle. Consequently, there is a potential for reducing errors in the clinical IOP tonometry.

## Original papers

This thesis is based on the following papers, which are referred to by their Roman numerals in the text. Papers I and II are reprinted with permission from the publishers.

- I. ANDERS EKLUND, ANDERS BERGH AND OLOF LINDAHL (1999): ‘A catheter tactile sensor for measuring hardness of soft tissue: measurement in a silicone model and in an *in vitro* human prostate model’, *Medical and Biological, Engineering and Computing*, **37**, pp. 618-624
- II. ANDERS EKLUND, TOMAS BÄCKLUND AND OLOF LINDAHL (2000): ‘A resonator sensor for measurement of intraocular pressure – evaluation in an *in vitro* pig-eye model’, *Physiological Measurement*, **21**, pp 355-367
- III. ANDERS EKLUND, CHRISTINA LINDÉN, TOMAS BÄCKLUND, BRITT ANDERSSON AND OLOF LINDAHL: ‘Evaluation of applanation resonator sensors for intraocular pressure measurement, results from clinical and *in vitro* studies’, *Submitted*
- IV. ANDERS EKLUND, PER HALLBERG, CHRISTINA LINDÉN, AND OLOF LINDAHL: ‘An applanation resonator sensor for measuring intraocular pressure using combined continuous force and area measurement’, *Submitted*

## List of abbreviations

$\rho$	= Density
$\beta_0, \beta_1$	= Coefficients in an ARS model
$\alpha$	= Acoustic resistance of an object
$\beta$	= Acoustic reactance of an object
$\Delta\phi_{SE}$	= Change of phase shift over sensor element
$\Delta f$	= Frequency shift of a rod resonance top
$\phi_{FC}$	= Phase shift over feedback circuit
$\Delta f_S$	= Frequency shift for resonator sensor system
$\phi_{SE}$	= Phase shift over sensor element
$\omega$	= Angular frequency
$\nu$	= Poisson's ratio
$A$	= Contact area
ARS	= Applanation resonator sensor
$C_{ARS}$	= Proportionality constant between frequency shift and area
$C_{Offset}$	= Constant
CTS	= Catheter tip tactile sensor
$C_x$	= Compliance related part of $\beta$
E	= Young's modulus
$f$	= Frequency
$f_0$	= Frequency of unloaded sensor
$f_1$	= Frequency of starting point for interval used in analysis
$f_2$	= Frequency of end point for interval used in analysis
$F_C$	= Contact force
GAT	= Goldmann applanation tonometry
GPIB	= General Purpose Interface Bus
IOP	= Intraocular pressure
$IOP_{ARS}$	= IOP according to applanation resonator sensor
$IOP_{GAT}$	= IOP according to Goldman applanation tonometer
$IOP_{SC}$	= IOP according to saline column
$IOP_{VC}$	= IOP measured in vitreous chamber
$l$	= Length of a rod
$L$	= Indentation of the cornea
$L_1$	= Indentation at beginning of the interval used in the analysis
$L_2$	= Indentation at the end of the interval used in the analysis
$L_p$	= Penetration depth
$m_x$	= Mass related part of $\beta$
$n$	= Number of observations
NCT	= Non-contact tonometers
$p$	= Probability value
PSA	= Prostate specific antigen
PZT	= Lead zirconate titanate

$r$	= Correlation coefficient
$r_0$	= Radius of catheter
$R^2$	= Degree of explanation of a model
Stiffness	= The ratio $F/L_p$ for the sensor applied to an object (OMATA and CONSTANTINOU, 1995)
$t$	= Time references to initial contact
$t_1$	= Starting time for interval used in analysis
$t_2$	= End time for interval used in the analysis
$T_{cornea}$	= Corneal thickness
$V_0$	= Equivalent sound velocity in the sensor element
$Z_0$	= Acoustic impedance of the sensor element
$Z_x$	= Acoustic impedance of an object



# Contents

<b>1</b>	<b>Introduction .....</b>	<b>13</b>
<b>2</b>	<b>Prostate hardness .....</b>	<b>17</b>
2.1	Anatomy of the human prostate .....	17
2.2	Prostate cancer .....	17
<b>3</b>	<b>Intraocular pressure .....</b>	<b>19</b>
3.1	Anatomy of the human eye .....	19
3.2	Glaucoma .....	21
3.3	Intraocular pressure measurement methods .....	21
<b>4</b>	<b>Sensor theory .....</b>	<b>25</b>
4.1	Resonator sensors in general .....	25
4.2	Piezoelectricity .....	25
4.3	Resonator sensor principle .....	27
4.4	Resonator sensors for diagnostic purposes .....	29
<b>5</b>	<b>Aims of the study .....</b>	<b>31</b>
<b>6</b>	<b>Review of papers .....</b>	<b>33</b>
6.1	Paper I .....	33
6.2	Paper II .....	33
6.3	Paper III .....	33
6.4	Paper IV .....	34
<b>7</b>	<b>Material and methods .....</b>	<b>35</b>
7.1	Resonator sensor system .....	35
7.2	Catheter tip sensor .....	36
7.3	ARS sensors .....	36
7.4	<i>In vitro</i> experimental set-up .....	37
7.5	IOP clinical set-up .....	39
<b>8</b>	<b>General results and discussion .....</b>	<b>41</b>
8.1	A contact area measurement device .....	41
8.2	A hardness measurement device .....	45
8.3	An intraocular pressure measurement system .....	48
<b>9</b>	<b>General summary and conclusions .....</b>	<b>59</b>
<b>10</b>	<b>References .....</b>	<b>61</b>
<b>11</b>	<b>Acknowledgements .....</b>	<b>67</b>
	<b>Papers I - IV</b>	



# 1 Introduction

Modern computer advancements open the door for new measuring and monitoring methods with possibilities of extensive and complex input data. Research in the medical field is continuously expanding the knowledge of how different physiological variables relate to each other and how they can be used for diagnostic purposes. A sensor is an essential part in a measurement system collecting data of a physiological variable. Sensors are therefore playing an increasingly important role in medical care. This dissertation deals with a new sensor technique for medical use. The applications are focused on the physiological variables of intraocular pressure (IOP) and tissue hardness.

Measurement of the IOP is a routine investigation in every eye department. The fluid system of the eye normally maintains an almost constant IOP at approximately 16 mm Hg (LEYDHECKER et al., 1958). Continuous formation of aqueous humour by the ciliary processes is balanced by the outflow through the trabecular meshwork and uveoscleral pathway. The IOP maintains the eye in a rigid shape and keeps a constant distance between cornea, lens and retina (GUYTON, 1991, TORTORA and GRABOWSKI, 1996), which is essential for the optical properties of the eye. Glaucoma is an eye disease that may be defined as a progressive optic neuropathy with characteristic changes of the optic nerve head and visual field. The aetiology is not completely understood, but one of the major risk factors is elevated IOP (SOMMER, 1989), and all treatment, this far, is focused on reduction of the IOP (LINDÉN, 1997). It is therefore important to have simple and reliable methods for measuring IOP, both for diagnostic purposes and for follow-up after treatment.

In the clinical setting measurement of IOP is performed in an indirect way where a force indents or flattens the cornea. The relationship between force and indentation/contact area is used to estimate the internal pressure. The Goldmann applanation tonometer (GOLDMANN, 1957) is currently the most valid and reliable method (CANTOR, 2000). Examples of other tonometers used are Schiøtz indentation tonometer (FRIEDENWALD, 1937), Tono-Pen which is a microprocessor-controlled, hand-held tonometer (MINCKLER et al., 1987) and non-contact applanation tonometers (FORBES et al., 1974) which use an air pulse to flatten the cornea.

Two review papers (WHITACRE and STEIN, 1993, DOUGHTY and ZAMAN, 2000) address a number of sources of errors with the current tonometric methods.

For example, the optical principle of Goldmann applanation is sensitive to astigmatism and the Tono-Pen has been shown to overestimate at low and underestimate at high IOP (MIDELFART and WIGERS, 1994, WHITACRE and STEIN, 1993, EISENBERG et al., 1998). Generally, there is a sensitivity to corneal thickness (DOUGHTY and ZAMAN, 2000, EHLERS et al., 1975). Therefore, further development and new methods in the area of clinical IOP measurement are needed.

Tissue composition and consistency are often changed by disease. For example, malignant tumours are generally harder than the surrounding tissue, and this is the reason why tumours often can be detected by palpation. In the female, breast cancers are detected as harder regions imbedded in surrounding normal gland. Suspicious areas in the breast can further be examined by mammography and biopsy. In the male, prostate cancer is often detected as a firm nodule in the prostate during rectal palpation. Prostate cancer is the most common cancer in men in the European Union and the USA. Only in the US 165,000 men are diagnosed with prostate cancer each year (US-DEPT-HHS-PUBL, 1993).

Prostate cancer is generally diagnosed by a high blood PSA (prostate specific antigen) level, rectal palpation, and ultrasound examination of the prostate followed by histological examination of prostate biopsies. In many patients with high PSA, palpation and ultrasound do not detect any tumour and biopsies are therefore taken at random (AARNINK et al., 1998, HODGE et al., 1989). Therefore, there is a need for improved, non-invasive methods to detect prostate tumours in a reliable and easy way.

In 1989 a tactile sensor based on vibration technology for measuring physical properties such as stiffness or hardness of an object was presented (OMATA, 1989). The system is based on a ceramic piezoelectric element set in oscillation with an electronic feedback circuit (OMATA and TERUNUMA, 1992). When the element touches an object with a certain acoustic impedance the resonance frequency of the oscillating system changes. Preliminary results from measurements of living tissue by detecting the change in frequency have given promising results (OMATA and TERUNUMA, 1991, LINDAHL et al., 1998). The tactile sensor technique has been evaluated both in a standardised silicone rubber model and in a rat testis model where it was compared with an impression method that measures interstitial pressure and water displacement in skin (LINDAHL and OMATA, 1995). It has also been evaluated for detection of changes in stiffness and elastic-related properties of the human skin (LINDAHL et al., 1998). The results of these studies suggest that the sensor probe with the

measuring instrument can measure differences in stiffness of silicone and is promising to provide information about the properties of skin stiffness and elasticity. Furthermore, a published study showed that lymph node stiffness measured with the tactile sensor was a useful parameter for diagnosis of metastases in an *in vitro* setting (MIYAJI et al., 1997). Another study with a catheter type tactile sensor in an animal model indicated that direct measurement of bladder stiffness may prove to be a useful tool in the evaluation of bladder and prostate biomechanics (WATANABE et al., 1997).

This dissertation investigated the theory and experimental results regarding frequency characteristics of the resonator sensor system described above, and how these characteristics are affected when the elements are set in contact with tissue of different kinds. A tissue hardness measurement application and an *in vitro* model for prostate tissue hardness measurement were proposed and evaluated in Paper I. Within the scope of this dissertation a new application and a new design for the sensor system has been proposed. Under certain conditions the sensor has proven to be a very sensitive device for measuring area of contact between sensor and sample as shown in Paper I. That sensor property has been utilised in a new measurement method for intraocular pressure. For evaluation of IOP tonometry methods an *in vitro* pig-eye model was developed. Papers II, III and IV describe the development, evaluation and modelling of the Applanation Resonator Sensor (ARS) for IOP measurement.



## 2 Prostate hardness

### 2.1 Anatomy of the human prostate

The prostate gland is a single, doughnut-shaped gland about the size of a walnut. It is inferior the urinary bladder and surrounds the prostatic urethra (Fig. 1) (TORTORA and GRABOWSKI, 1996, MOORE, 1992). The normal prostate is partly glandular and partly fibromuscular. Secretion from the prostate gland enters the prostate urethra through many prostatic ducts. The secretion makes up about 25% of the semen and contributes to sperm motility and viability.

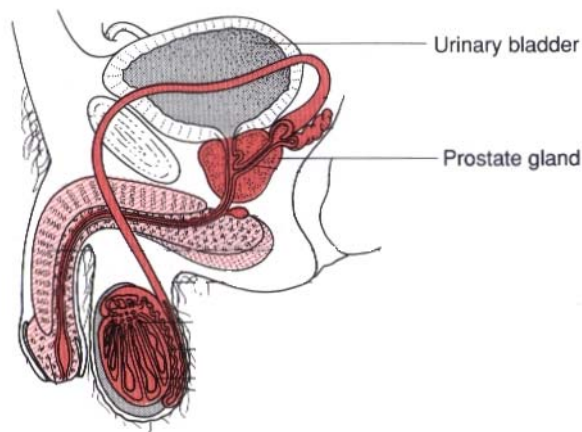


**Figure 1.** The prostate gland. Modified from Guyton (1991).

### 2.2 Prostate cancer

Prostate cancer is the most common cause of death from cancer in men in the United States (TORTORA and GRABOWSKI, 1996). A blood test can measure the level of prostate-specific antigen (PSA) in the blood. This substance is an enzyme produced only by prostate epithelial cells. The amount of PSA increases with enlargement of the prostate gland and may indicate infection, benign enlargement, or prostate cancer. Tissue composition and consistency are often changed by disease. For example, malignant tumours are generally harder than the surrounding tissue. Examination of the prostate gland can therefore be performed by a digital rectal exam, in which the physician palpates the gland through the rectum with a finger. Transrectal ultrasonography, where a rectal ultrasound probe is used to image the prostate, is also used to detect tumours (TORTORA and GRABOWSKI, 1996). These investigations are followed by prostate biopsy. In many patients with high

PSA, palpation and ultrasound do not detect any tumour and biopsies are therefore taken at random (AARNINK et al., 1998, HODGE et al., 1989). Therefore, there is a need for improved, non-invasive methods to detect prostate tumours in a reliable and easy way. Maybe, a method for measuring tissue hardness in an objective way could be used to guide the physician when taking biopsies in areas suspicious for cancer. Treatment of prostate cancer involves surgery, radiation, hormonal therapy and chemotherapy.

## **3 Intraocular pressure**

### **3.1 Anatomy of the human eye**

The adult eyeball is about 25 mm in diameter (TORTORA and GRABOWSKI, 1996, MOORE, 1992). The wall of the eyeball can be divided into three layers, a fibrous tunic, a vascular tunic and the retina, which is a nervous tunic (Fig. 2). The fibrous tunic is the superficial coat and consists of the anterior cornea and the posterior sclera. The cornea is a nonvascular, transparent coat with surfaces of squamous epithelium and a middle layer with collagen fibers and fibroblasts. The corneal thickness is approximately 0.53 mm (DOUGHTY and ZAMAN, 2000). The sclera is the white of the eye, and is a coat of dense connective tissue made up mostly of collagen fibers and fibroblasts. The sclera covers the entire eyeball except the cornea, and it gives the shape of the eyeball and makes it rigid.

The vascular tunic, or uvea, is the middle layer of the wall and contains choroid, ciliary body and iris. The highly vascular choroid lines the inner surface of the sclera and provides nutrients to the retina. In the anterior portion the choroid becomes the ciliary body. The ciliary body consists of a ciliary muscle that alters the shape of the lens for focus and the ciliary processes which contain blood capillaries that secrete a watery fluid called aqueous humor. The iris is the coloured portion of the eyeball that regulates the amount of light entering into the eye through the pupil. The inner coat of the eyeball is the retina, which lines the inner three-quarters of the eyeball and is the beginning of the visual pathway. The retina is a thin delicate membrane composed of two layers, a light sensitive neural layer and an outer pigment cell layer. The optic disk (head) is the site where the optic nerve exits the eyeball.

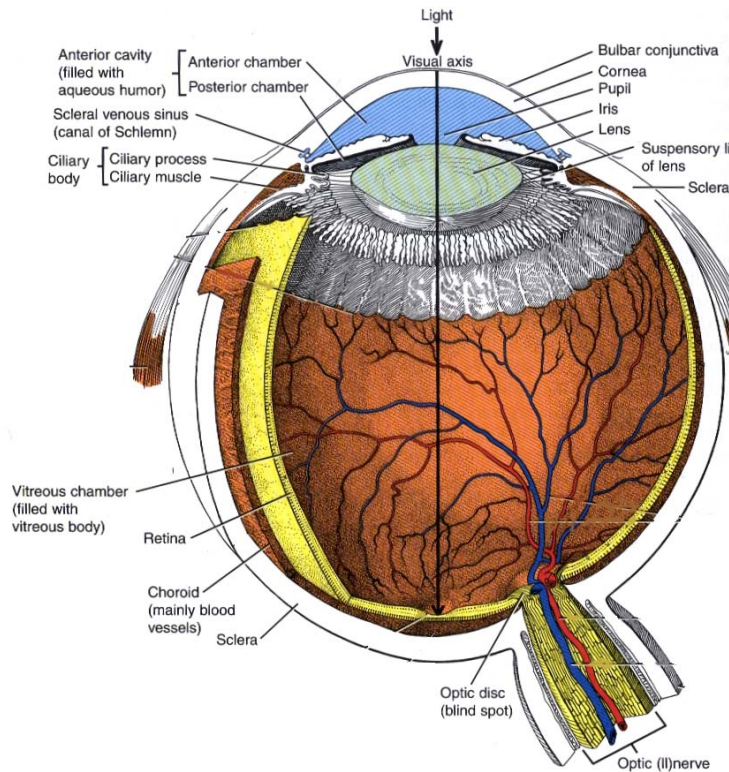


**Figure 2.** The anatomy of the eye. Modified from Tortora and Grabowski (1996).

The interior of the eyeball is a space divided by the lens into two cavities, the anterior cavity, with the anterior and posterior chamber, and the vitreous chamber. The vitreous body is a jellylike substance that fills out the vitreous chamber. The substance contributes to prevent the eyeball from collapsing.

The anterior cavity is filled with aqueous humour that is continually filtered from the ciliary processes and reabsorbed into the venous blood. It is the balance between formation and reabsorption of the aqueous humour that regulates the total volume and pressure of the intraocular fluid (GUYTON, 1991). The formation rate is approximately 2-3  $\mu$ l per minute and is almost entirely an active secretion. After formation the aqueous humour flows from the posterior chamber through the pupil and into the anterior chamber of the eye. Here the fluid exits the eye into the angle between the cornea and the iris and through the trabecular meshwork, finally entering into the canal of

Schlemm, which empties into the extraocular veins. A minor part of the aqueous humour leaves the eye through the uveoscleral pathway.

Normal intraocular pressure (IOP) is approximately 16 mm Hg (LEYDHECKER et al., 1958), and remains very constant in the normal eye, normally within about  $\pm 2$  mm Hg (GUYTON, 1991). The level of this pressure is determined by the formation rate and the resistance to outflow of aqueous humour from the anterior chamber into the canal of Schlemm. The main resistance is in the trabecular meshwork of, which only have minute openings of 2 to 3  $\mu\text{m}$ .

### **3.2 Glaucoma**

Glaucoma is an eye disease that may be defined as a progressive optic neuropathy with characteristic changes of the optic nerve head and the visual field (LINDÉN, 1997). The aetiology is not completely understood, but one of the major risk factors is elevated intraocular pressure (IOP). The relative risk for glaucomatous optic nerve damage is shown to be 10 times higher for patients whose IOP exceeded 23 mm Hg, compared to those with IOP below 16 mm Hg (SOMMER, 1989). Open-angle glaucoma is a painless insidious disease. As long as the other eye is not affected, a person may experience considerable retinal damage and visual loss before the condition is diagnosed (TORTORA and GRABOWSKI, 1996). The disease affects 5% of people over 65 years (TORTORA and GRABOWSKI, 1996). All treatment, so far, is aimed at reducing IOP. The reduction of IOP is done by reducing the production of aqueous humour or by increasing the outflow. Both pharmaceutical and surgical methods are available. Therefore, for diagnostic purposes and for follow-up after treatment, it is important to have simple and reliable methods for measuring the IOP. Today, tonometry is a standard procedure in all examinations of the eye.

### **3.3 Intraocular pressure measurement methods**

#### **3.3.1 History of tonometry**

The first clinical applanation tonometers were introduced by WEBER (1867) and MAKLAKOFF (1885). The Maklakoff tonometer estimated the area of cornea that was flattened by a cylinder of known weight. IMBERT (1885) discussed the forces relevant to tonometry and gave a formula stating that the pressure exerted by a tonometer against the globe was equal to IOP plus the adhesion produced by surface tension forces. FICK (1888) repeated the hypothesis that if a small segment of a sphere was flattened the force flattening the sphere

corresponded to the pressure within the sphere. Shciøtz introduced his indentation tonometer in 1906, which was then generally adopted as the most useful tonometer (FRIEDENWALD, 1937). In 1954 the more accurate Goldmann applanation tonometer (GOLDMANN, 1957) was presented and it is still the most popular instrument for measurement of intraocular pressure (OTTAR, 1998).

### 3.3.2 Imbert-Ficks law

For IOP measurement the applanation principle is generally described through the Imbert-Fick law (WHITACRE and STEIN, 1993). It states that when a flat surface is pressed against a spherical surface of a container with a given pressure, an equilibrium will be attained in which the force,  $F_C$ , exerted against the spherical surface is balanced by the internal pressure,  $IOP$ , of the sphere exerted over the area of contact,  $A$ , between the sphere and flat surface. That is:

$$F_C = IOP \cdot A \quad (1)$$

It is assumed that the sphere applanated by the flat surface is infinitely thin, perfectly elastic, perfectly flexible and that the only force acting against it is the pressure of the applanated surface. It is further assumed that the applanated area and subsequently the displaced volume is small in relation to the total area and volume of the sphere.

### 3.3.3 Goldmann applanation tonometer

The Goldman applanation tonometer (GAT) is considered the most valid and reliable method for measuring the IOP (CANTOR, 2000). In short the set-up contains an optical head with a special prism. This head is mounted on a force balance, which in turn is mounted on a biomicroscope. The flat contact surface of the optical head is pressed against the cornea. The operator adjusts the contact force with the force balance. A predefined contact area is obtained by adjusting the force until a certain pattern is viewed with the microscope through the prism. With a predefined area the IOP can be deduced from the contact force  $F_C$  according to equation(1). Thorburn has shown that the 95% confidence interval for the difference between two consecutive IOP measurements with GAT done by the same observer was  $-0.5 \pm 1.7$  mm Hg (THORBURN, 1978). For measurements performed by different observers the interval increased to  $-0.7 \pm 3.1$  mm Hg.

### 3.3.4 Guard ring tonometers

The applanation method with a guard ring was proposed MACKAY and MARG (1959). The applanating surface is divided into a central part and a

guard ring part, and the force is measured in the central part of the contact surface. Tono-Pen is a hand-held guard ring applanation tonometer that uses a micro strain gauge transducer to measure the force on a central plunger with a diameter of 1.02 mm (MINCKLER et al., 1987). The guard ring has a 3.22 mm diameter. The output from the force transducer when the cornea is applanated is analysed by an on-board microprocessor and the IOP is calculated. Evaluation of Tono-Pen and ProTon, which is a similar instrument, in comparison to GAT has shown that the 95% limits of agreement between GAT and Tono-Pen are between  $-3$  to  $+8$  mm Hg and between GAT and ProTon  $-4$  to  $+5$  mm Hg (MIDELFART and WIGERS, 1994).

### 3.3.5 Pneumatometer

The principle of the pneumatometer, developed by Langham and co-workers, has been described by MOSES and GRODZKI (1979). It is based on a gas-operated servo system that propels a plunger, with air outflow through a special membrane tip, against the cornea. The outflow of gas is impeded at contact, resulting in a pressure rise in the flow system and an increased force on the plunger. This way a gas-operated servo system exists in which the force of the plunger against the cornea is governed by the pressure in the gas flow system. The equilibrium pressure of the system is recorded, and it is proportional to the IOP. In a comparison study (QUIGLEY and LANGHAM, 1975) with GAT, 85% of the measurements were within  $\pm 3$  mm Hg ( $n=100$ ).

### 3.3.6 Non-contact tonometers

Non-contact tonometers (NCT), based on the applanation principle, that measures the IOP without touching the eye, have been developed (FORBES et al., 1974). A central area of the cornea is deformed by a controlled air pulse of linearly increasing force impinging on the cornea. A monitoring system senses the light reflected from the corneal surface and records the maximal signal at the instant of applanation. In a comparative study with GAT, Forbes et al. showed a correlation of 0.9 and a SD of 2.86 mm Hg ( $n=570$ ) between the methods for differences between pairs (FORBES et al., 1974). Seven more recent studies, partly summarised by Hansen (HANSEN, 1995), where NCT air-puff tonometers were compared with GAT, have shown a wide range of SD (1.12 to 2.93 mm Hg) for the difference between methods (HANSEN, 1995, PARKER et al., 2001).

### 3.3.7 Schøitz tonometer

The Schøitz method measures how deep a certain weight will indent the cornea (FRIEDENWALD, 1937). The lower the IOP the greater the indentation. The instrument is placed on the cornea with a foot plate. The weight is placed

on a plunger and on a scale the operator can read the depth of the indentation. From calibration tables IOP in mm Hg can be estimated from the scale value and the weight.

## **4 Sensor theory**

### **4.1 Resonator sensors in general**

JORDAN (1985) suggested a general definition of resonator sensors. They are devices based upon a principle whereby the resonant frequency or frequency distribution produced in a mechanical structure is measured and related to the physical property to be determined. In the sensor system there is a need for an electronic drive circuit that maintains the oscillations; the frequency characteristics of this circuit will also affect the resonance frequency. A resonator sensor can use variable stress in a mechanical structure to cause a change in its resonance frequency (LANGDON, 1985). For example, a stretched string connected to a diaphragm will change its tension depending on the pressure on the diaphragm (JORDAN, 1985). Other resonator principles are sensors that are affected by change in the system inertia with a mass change or change in surrounding material. There are sensors for measuring liquid level or liquid/gas density based on that principle (STEMME et al., 1983, LANGDON, 1980). Decay time and phase variations are also examples of parameters that can be used in a resonator sensor system. Viscosity has long been measured with this technique (LANGDON, 1985).

Many resonator sensors use piezoelectric transducers mounted on the vibrating element to drive the oscillation and for pick-up of the vibration. In some cases the whole vibrating element is made of quartz or a ceramic piezoelectric material. The advantage of the piezoelectric material is that they enables the vibration to be maintained and measured by a simple electrical drive circuit.

### **4.2 Piezoelectricity**

The piezoelectric effect was discovered in 1880 by Pierre and Jacques Curie (IKEDA, 1990). Piezoelectricity involves the interaction between mechanical and electrical behaviour of the medium. The direct piezoelectric effect is that electric polarisation is produced by mechanical stress, and the inverse piezoelectric effect is that the same materials deform when they are exposed to an electric field. The piezoelectric effect is found in naturally occurring crystals like quartz and tourmaline (WAANDERS, 1991).

For a crystal to exhibit this effect its structure should have no centre of symmetry. A stress applied to the crystal will alter the separation between positive and negative charge sites in each elementary cell, leading to a net

polarisation at the crystal surface. This generates an electric field and a voltage over the crystal. The effect is practically linear and also reciprocal, that is, if the crystal is exposed to an electric field it will experience an elastic strain causing its length to increase or decrease according to the field polarity.

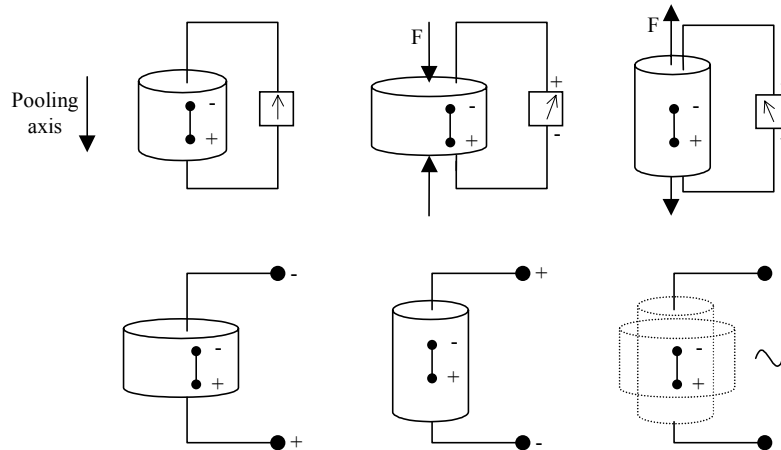


**Figure 3.** Example of the piezoelectric effect in a cylindrical element.  $F$  is the applied force to the body. The pooling axis and the dipoles shows the polarisation in the element. For ceramic piezoelectric material the pooling direction is determined in the manufacturing process by applying a strong electric field in that direction. The upper pictures shows how an electrical potential, symbolised by voltmeters, is generated over the elements from deformation due to an applied force. The lower row of pictures shows how a deformation is generated by applying an electrical voltage over the element. A sinusoidal voltage variation will cause the element to oscillate.

Piezoelectric elements can also be produced in ceramic material (WAANDERS, 1991). The sensor elements used in the studies presented in this dissertation were based on a ceramic piezoelectric material. These materials can be considered as a mass of minute crystallites. Below the Curie temperature the elementary cell of these crystallites is not centrosymmetric, which creates a dipole. Neighbouring dipoles align with each other to domains of local alignment. The ceramic is then made piezoelectric in a chosen direction by heating the sample to just below the Curie temperature and adding a strong electric field in that direction. This will make the domains with dipoles in the field direction to grow on the expense of the domains with dipoles in other directions. When the electric field is turned off the dipoles remain locked in the approximate direction of the field, and there will be a net dipole moment and a remanent polarisation. There will also be a permanent deformation related to the polarisation. The ceramic piezoelectric element will

now act the same way as the piezoelectric crystal; with a voltage over the sample if a force is applied, and with a deformation if a voltage is applied (Fig. 3). Lead Zirconate Titanate (PZT) is a ceramic piezoelectric material.

### 4.3 Resonator sensor principle

In the work of this dissertation a new type of resonator sensor was further developed and evaluated. The sensor technique was first presented by OMATA (1989). Three years later, OMATA and TERUNUMA (1992) presented the basic description of this resonator sensor system. It is based on a ceramic piezoelectric element shaped like a rod or cylinder, made out of PZT and with a piezoelectric pick-up. When an alternating voltage is applied across its electrodes the element will vibrate freely in the direction of its length. The pick-up detects the vibration and feeds the alternating signal to a driving amplifier in a feedback circuit. The circuit drives the PZT-element and the system oscillates at its resonance frequency. If the free end of the PZT-element, or a contact piece attached to that end, touches an object the resonance frequency characteristics and frequency of the system will change (Fig. 4). The amount of change depends on the acoustic impedance of the object. The sensor system output signal is the shift of the oscillation frequency from unloaded to loaded condition.

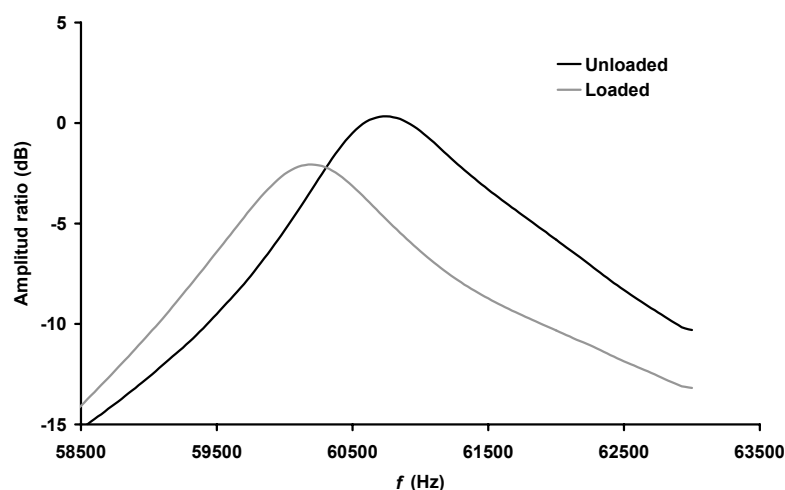


**Figure 4.** The amplitude frequency response characteristics for the sensor probe used in Paper IV. Black curve displays the unloaded sensor and grey curve the response when the sensor was applied to a silicone sample. The figure shows how the whole frequency characteristic curve shifts to a lower frequency when the sensor is applied to the sample. It is, in principle, this shift that can be detected with the resonator sensor system.

### 4.3.1 Mechanical oscillations in a rod

The behaviour of the sensor system can be explained and approximated in terms of the vibration mode of a finite rod (OMATA and TERUNUMA, 1992). If the end of a finite rod of length,  $l$ , is attached to an unknown impedance,  $Z_x$ , the theoretical treatment of a vibrating rod will predict the change in resonance frequency from unloaded to loaded condition as:

$$\Delta f = -\frac{V_0}{2\pi l} \frac{\beta}{Z_0} \quad (2)$$

where  $Z_0$  is the acoustic impedance of the sensor element and  $V_0$  is the equivalent sound velocity in the sensor element.  $\beta$  is the reactance of the unknown impedance  $Z_x$ :

$$Z_x = \alpha + j\beta \quad (3)$$

with  $\alpha$  as the resistive load. The reactance,  $\beta$ , can be further divided into a mass load part, described with  $m_x$ , and a compliance term, described with  $C_x$ :

$$\beta = \omega m_x - \frac{1}{\omega C_x} \quad (4)$$

where  $\omega$  is the angular frequency. The two parts will depend on material properties of the measured object. OMATA and TERUNUMA (1992) also suggested that both  $m_x$  and  $C_x$  are related to the contact area,  $A$ , between the sensor and the object:

$$m_x = \frac{\rho A^{3/2}}{10(1-\nu)} \quad (5)$$

$$C_x = \frac{1}{2} \sqrt{\frac{\pi}{A}} \frac{1-\nu^2}{E} \quad (6)$$

where  $\rho$  is density of the object,  $\nu$  is Poisson's ratio and  $E$  is Young's modulus.

#### **4.4 Resonator sensors for diagnostic purposes**

In the original paper OMATA and TERUNUMA (1992) demonstrated that a tactile sensor using the resonator technique was capable of sensing characteristics like change in elasticity of the skin and muscle caused by acupuncture therapy. They concluded that for applications based on the new sensor, a lot of difficulty remained to be solved, but the feature of the sensor was that it could sense hardness or softness of an object like the human hand does. Since then, a number of tactile sensors based on the resonator sensor technique have been developed and evaluated by Omata and co-workers.

To measure oedema, the tactile sensor technique has been compared to an impression technique (LINDAHL and OMATA, 1995). In that study, the evaluation was performed in a silicone rubber model and in a rat testis model. They found that frequency shift of the resonator sensor correlated with the established impression parameters for describing hardness of living tissue. Furthermore, their results (LINDAHL and OMATA, 1995) indicated that frequency shift of their resonator sensor linearly related to softness of silicone according to an International standard (DIN ISO 2137).

It has been shown that small invisible nodules, that cannot be detected from the lung surface, in patients undergoing thorascopic operation, were located successfully using a tactile sensor applied on a rod (OHTSUKA et al., 1995). In another study (MIYAJI et al., 1997), measurement of stiffness with a catheter type resonator sensor mounted in a counter balance arrangement (constant weight 2 g) and applied to resected lymph nodes from patients that underwent lobectomy or pneumonectomy was performed. Their study confirmed that stiffness, according to the frequency shift of the sensor, is an accurate approach to diagnose lymph node metastases.

In another study with a tactile sensor mounted in a counterbalance arrangement, it was shown that the stiffness of excised rat prostate varied after hormone treatment and could be differentiated using the sensor (OMATA and CONSTANTINOU, 1995). They also showed in a gelatin model that change in frequency could be calibrated against stiffness of gelatine, calculated from the counterweight and the depression (OMATA and CONSTANTINOU, 1995). Bladder wall compliance based on cystometry was compared with stiffness measurement with a resonator sensor in another rat model study (WATANABE et al., 1997). The findings indicated that the direct measurement of bladder wall stiffness may be a useful tool in the evaluation of bladder and prostate biomechanics.

Lindahl et al. evaluated a tactile sensor for stiffness and elastic properties of human skin (LINDAHL et al., 1998). From measurements on 874 women's cheek's skin, they concluded that the sensor system is promising for providing information on skin stiffness and elasticity.

In summary, the studies referred to above points towards a potential in the new sensor technique. However, the basic relationships between frequency shift and the physical parameters under investigation are not fully understood(LINDAHL and OMATA, 1995), and the general opinion is that further research are needed (OMATA and TERUNUMA, 1992, LINDAHL and OMATA, 1995, WATANABE et al., 1997, LINDAHL et al., 1998).

## 5 Aims of the study

The aims of this study were:

- to determine which physical variables a resonator sensor will sense when it is applied to an object, and how these variables relate to changes in the measured resonance frequency.
- to take a first step towards a non-invasive method for prostate cancer measurement, by developing an *in vitro* hardness measurement method using a catheter type tactile sensor and evaluate it on silicone samples and prostate tissue.
- to develop an applanation resonator sensor (ARS) for measurement of IOP, and also to develop an *in vitro* model with which tonometry methods could be evaluated.
- to further develop and evaluate the ARS system, in a clinical study and in an *in vitro* study, in order to improve the measurement accuracy towards a clinical application.
- to develop a new IOP measurement method based on a continuous force and area recording during the initial applanating phase, and to further develop and evaluate the ARS system according to this new method.



## 6 Review of papers

### 6.1 Paper I

A catheter-type tactile sensor based on resonator sensor technique was evaluated in a silicone model and applied to human prostate *in vitro*. The main finding was that different histological compositions of prostate tissue correlated with the frequency shift of the resonator sensor and that the common property was the hardness of the tissue. The results indicated that hardness of the prostate tissue, and maybe hardness of human tissue in general, can be expressed according to a cone penetration standard (DIN ISO 2137) and that the hardness can be measured with this tactile sensor system. The tissue hardness application for the resonator sensor technique is yet to be further developed and evaluated in a larger study. This paper also produced a number of results that have led to the basic understanding of the resonator sensor system. One important result was that change in contact area was correlated to change in phase shift over the resonator element. Frequency shift of the sensor system, in turn, was shown to depend on this phase shift through the zero phase resonance condition. This indicated that the resonance sensor could be used for area measurement.

### 6.2 Paper II

In this paper the applanation resonator sensor (ARS) for measurement of intraocular pressure (IOP) was introduced and evaluated. For this purpose an *in vitro* pig-eye model was developed, and it was shown that a saline column connected to the vitreous chamber of the pig-eye could be used successfully to induce variations in IOP. The sensor was applied against the cornea with constant force and frequency shift was measured. A mathematical model based on the Imbert-Fick law and the assumption that frequency shift was linearly related to contact area was proposed and verified with convincing result. IOP measured with the resonator sensor correlated well ( $r=0.92$ ,  $n=360$ ) with the IOP elicited by the saline column.

### 6.3 Paper III

The ARS in constant force application was evaluated on healthy *in vivo* human eyes. The results verified the sensor principle but revealed a non-negligible source of error in off-centre positioning between the sensor and the cornea. The sensor probe was redesigned and evaluated with the *in vitro* pig-

eye model. The new probe, with a spherical contact surface against the eye, reduced the sensitivity to off-centre positioning. It was also showed that a frequency shift normalisation procedure could reduce the between-eye differences. It was concluded that a spherical contact surface should be preferred and that further development towards a clinical instrument should focus on probe design and signal analysis.

#### **6.4 Paper IV**

The applanation resonator sensor method for IOP measurement was further developed using combined continuous force and area measurements during the dynamic phase when the sensor initially applanates the cornea. A force sensor was included with the resonator sensor in one probe. Evaluation was performed with the *in vitro* pig-eye model. The hypothesis was that the IOP could be deduced from the differential change of force and area during initial applanating phase. There was good accuracy and good reproducibility with a correlation of  $r=0.994$  ( $n=414$ ) between measured pressure in the vitreous chamber and IOP according to the ARS. Measurement time was short, 77 ms after initial contact. Problems with between-eye differences and low resolution at high pressures were reduced. The ARS method is the first to combine simultaneous, continuous sampling of both parameters included in the applanation principle. Consequently, there is a potential for reducing errors in the clinical IOP tonometry.

## 7 Material and methods

### 7.1 Resonator sensor system

The resonator sensors used in this dissertation were based on vibrating piezoelectric elements shaped in the form of a rod or a cylinder and made out of Lead Zirconate Titanate (PZT). The elements had a piezoelectric pick-up for detection of the vibration. In each probe, the element was set in oscillation, at its resonance frequency, by means of an electronic feedback circuit (Fig. 5). This signal was first processed in a feedback circuit and then used for excitation of the PZT element. The feedback circuit modified the sinusoidal signal: first the signal was amplified to a constant amplitude signal, so that only the frequency and phase information of the signal were transferred. Then the signal was filtered in a band-pass filter to ensure that the PZT element would oscillate in its lowest longitudinal mode. The oscillator frequency was thus solely determined by the zero-phase condition; the sum of the phase shifts around the feedback loop (feedback circuit and PZT element) must be zero (FLOYD, 1988).

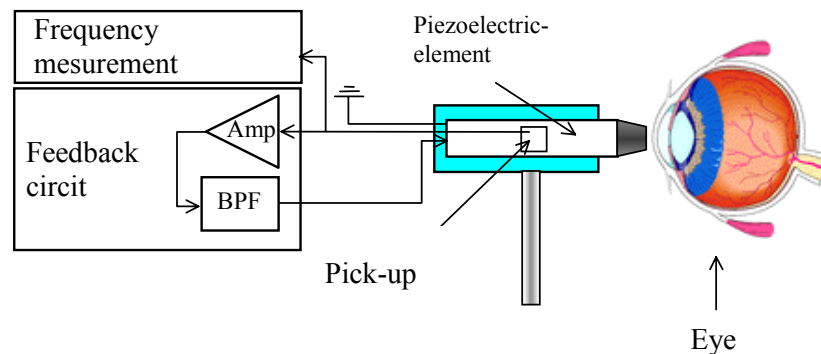


**Figure 5.** Resonator sensor system showing the principle, in an example for measurement of eye pressure. The feedback circuit consists of an amplifier (Amp) and a band-pass filter (BPF).

The system output signal is the shift of the oscillation frequency from unloaded to loaded condition, denoted  $\Delta f_s$ . As described in Paper I, the  $\Delta f_s$  will be dependent on the acoustic impedance of the load, the frequency characteristics of the unloaded sensor element and the frequency characteristics of the feedback circuit through the zero-phase condition. In the studies included in this dissertation four different resonator sensor probes based on this technique have been used.

## 7.2 Catheter tip sensor

The catheter tip tactile sensor CTS (prototype by Axiom Co Ltd., Koriyama, Japan) was based on a cylindrical piezoelectric element made out of PZT,  $7 \times \varnothing 1.2$  mm, placed at the end of a catheter with a radius of  $r_0 = 1.0$  mm. An integrated part of the element was used as a pick-up. At the tip, in contact with the element, a hemisphere of epoxy was placed, which sealed the catheter. Its fundamental resonance frequency was approximately 200 kHz.

## 7.3 ARS sensors

The first two applanation resonator sensors (ARS) used a rod-shaped ( $25 \times 5 \times 1$  mm) PZT element. A small PZT pick-up glued on to the PZT element detected the vibrations. One end of the rod was tapered and a specially shaped contact piece of nylon was fitted and glued onto the end. The element was mounted with foam rubber in a plastic cylinder (Fig. 6).

For the first probe, the contact piece was formed as a hemisphere with a flat end ( $\varnothing = 7$  mm) towards the cornea, this probe will be denoted flat probe (Fig. 6, left) (Papers II and III). For the second probe a spherical contact piece with a diameter of 4.6 mm was glued to the end (Fig. 6, right). This probe will be denoted spherical probe (Paper III). The resonance frequency of the unloaded oscillating system was approximately 82 kHz for the flat probe and 66 kHz for the spherical probe.



**Figure 6.** The flat ARS probe and spherical ARS probe.

The third ARS probe (Paper IV) consisted of a non-tapered PZT rod shaped ( $23 \times 5 \times 1$  mm). A bakelite piece, used for contact against the cornea, was glued onto one end of the PZT element. The contact surface of the piece was convex with a 7 mm radius of curvature. The sensor was mounted with a plastic suspension and placed in a sensor module together with a force transducer (Fig. 8). Resonance frequency was approximately 61 kHz.

## 7.4 *In vitro* experimental set-up

All four papers (I to IV) for evaluating the resonator sensor principle included *in vitro* measurements. The experimental set-up for this purpose has undergone a continuous development during the course of this work. The basic arrangement is shown in Figure 7. In the early papers (Papers I, II and III) conventional instruments, frequency counter and balance were used, and data were recorded into the computer through a GPIB and RS 232 interfaces. This system supported precise measurements of “steady state” conditions of frequency shift and contact force. Sampling rate was 1 to 10 Hz. In Paper III, a frequency-to-DC-voltage converter based on a phase-locked loop circuit was developed to facilitate data-acquisition of frequency with a data acquisition card and a sampling rate of 1 kHz.

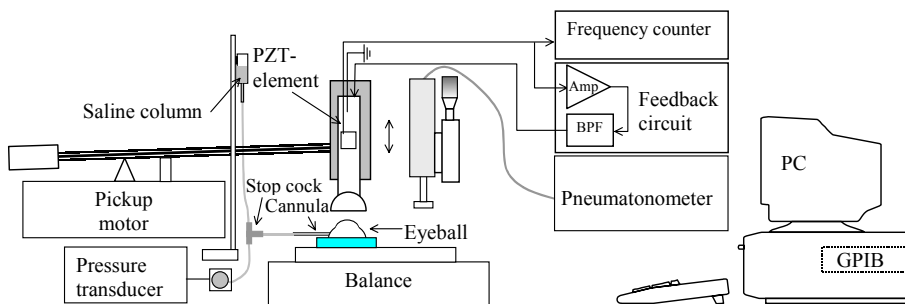


**Figure 7.** Experimental set-up for the measurements in Papers II, III and IV. With exception of the pressure-related parts and with the addition of a z-translator for controlled penetration depth, the same set-up was, in principle, used in Paper I for measurement on prostate tissue and silicone samples. The resonator sensor probe varied between studies. The counter balance arrangement was used for constant contact force,  $F_C$ , application. The pneumatometer was only used in Paper II.

Finally, for Paper IV, the set-up was extended with an inductive indentation measurement device and a built-in force transducer in the probe (Fig. 8). The experimental set-up could now be used to continuously record frequency, force and indentation in a way that made it possible to closely evaluate the fast dynamic phases such as the initial appanation phase when the sensor was applied to the cornea.

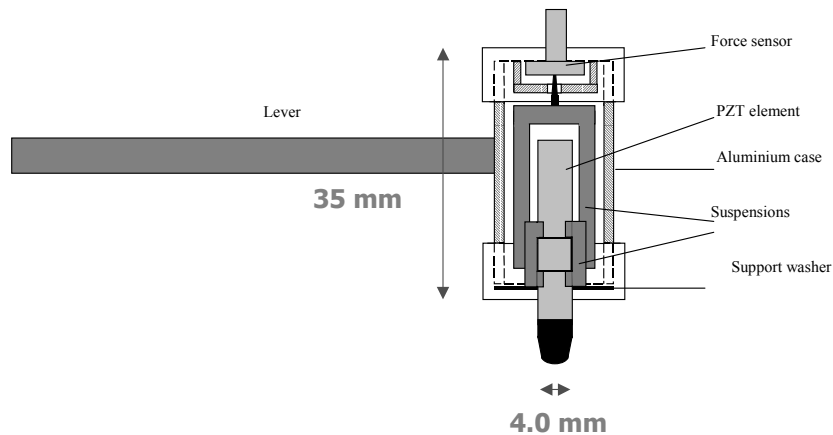


**Figure 8.** For the experimental set-up of Paper IV a new sensor module for ARS IOP measurement was developed. The module consisted of a resonator element for area measurement mounted on a force transducer. Indentation was measured with an inductive position gauge on the lever. In this study a controlled indentation and measured-force method was used.

#### 7.4.1 Silicone model and prostate tissue

The CTS was evaluated in a silicone model and on human prostate *in vitro*. For the silicone model a two-component silicon, Wacker SilGel 612 (Wacker-Chemie GmbH, München, Germany) was used. It was poured into standard Petri dishes. The silicone was vulcanised into 5 samples of different hardness by changing the mixing ratio. For the *in vitro* human tissue measurements, prostate tissue was removed from a 72-year-old man suffering from benign prostate hyperplasia. A slice of the prostate, about 10 mm thick, was fixed in formalin for 24 h (TOBOCMAN et al., 1997), then stored in 50% ethanol. The tissue was used for evaluation of the CTS and for histological diagnosis.

#### 7.4.2 IOP Pig-eye model

Eyes from 3 to 6-month-old Landrace pigs were enucleated immediately after the pigs were put to death, either after completed surgery related to another research project (Papers II and III), or at the abattoir (SQM, Skellefteå, Sweden) (Papers III and IV). The eyes were mounted firmly in a petri dish with agar solution (15 g/l) that covered the eye to about 50%. A winged, thin-walled cannula  $\varnothing 0.8 \times 19.0$  (Terumo Corp., Tokyo, Japan) was introduced through the side of the eyeball into approximately the middle of the vitreous chamber (Fig. 7). The hole around the cannula was sealed with cyanoacrylate adhesive to avoid leakage (EISENBERG et al., 1998). The cannula was connected to a saline column consisting of PVC tubing, a three-way stopcock, and at the distal end a partially saline-filled syringe open to air. The

syringe was movable mounted on a stable stand. The eye was pressurised for 10 seconds by opening it to saline column. The pressure level was calculated from the measured height of the saline column,  $IOP_{SC}$ . Just before measurement the stopcock was closed to create a closed system that approximated the normal state of the eye (EISENBERG et al., 1998). The IOP was measured both with the applanation resonator sensor,  $IOP_{ARS}$ , with a pneumatonometer (Paper II), and with a standard pressure transducer connected to the infusion line,  $IOP_{VC}$ . To avoid drying of the cornea the eye was moistened before every pressurisation with room-tempered saline. To simulate blinking the saline was applied onto the eye with one sweep of a very soft goat-hair brush, Kreatima 922 (Schormdanner Pinsel, Nürnberg, Germany).

### **7.5 IOP clinical set-up**

In Paper III, a clinical evaluation of a flat-surfaced resonator sensor with constant contact force against the cornea was performed. A standard biomicroscope with the force balance of the GAT set-up was used. The flat resonator sensor probe was mounted in the position of the optic head used in standard GAT measurements. The force balance was fixed at a setting corresponding to 15 mN of contact force,  $F_C$ . Frequency was measured with a universal counter and recorded into a PC with 10 Hz sampling frequency. A total of 24 volunteers, 4 male and 20 female, participated in the study. Their median age was 46 years, range 16 to 56 years. All subjects were healthy. Measurements were taken on both eyes and additionally one time on one eye after massage. GAT was used as a reference method.



## 8 General results and discussion

### 8.1 A contact area measurement device

Prior to the start of the research project presented in this dissertation the resonator sensor had been presented as a tactile sensor like the human hand (OMATA and TERUNUMA, 1992). The frequency shift,  $\Delta f_S$ , of the sensor system was shown to detect differences in hardness or softness of a measured object in a general way. One of the aims was to determine what physical parameters the sensor could sense, and how these affected the frequency characteristics of the sensor system and thereby created a change in the easily measured resonance frequency.

In Paper I, this work was initiated by measuring on well-defined silicone samples. A resonator sensor element, mounted in a catheter, was isolated from the feedback loop and its phase-frequency characteristics were determined by driving the element with a frequency generator and measuring of phase shifts with a universal counter.

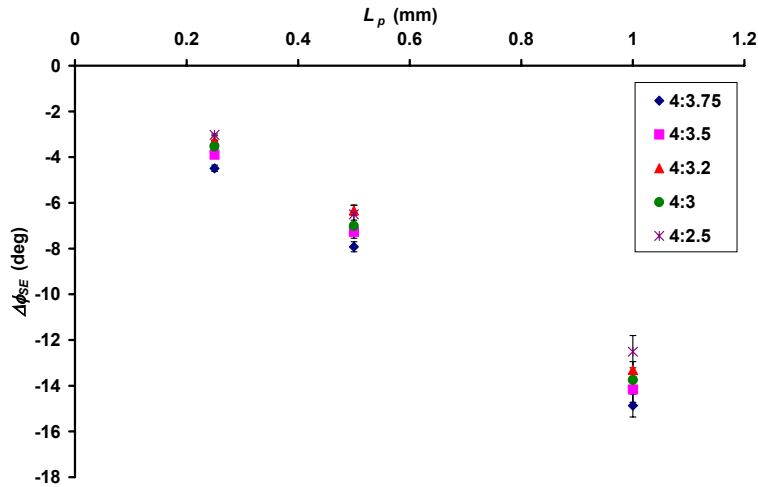


**Figure 9.** Change in phase shift from unloaded to loaded condition,  $\Delta\phi_{SE}$  (mean  $\pm$  SEM,  $n=10$ ), for a CTS-element, as a function of three penetrations,  $L_p$ . Measurements were done on five silicone samples of different hardness. The hardness presented by mixing ratio of the silicone, the higher the ratio the harder the silicone. The driving frequency was fixed at 190 kHz. The slope of the curves are approximately the same for all levels of hardness. (Data from Paper I).

It was shown that change in phase shift,  $\Delta\phi_{SE}$ , over the resonator element, in that case the catheter tip sensor (CTS) with a spherical contact surface, was linearly related to the penetration depth,  $L_p$ , into silicone samples of different hardness (Fig. 9). It was also shown that the slopes of the relations were independent of sample hardness (with exception of the hardest sample) (Paper I).

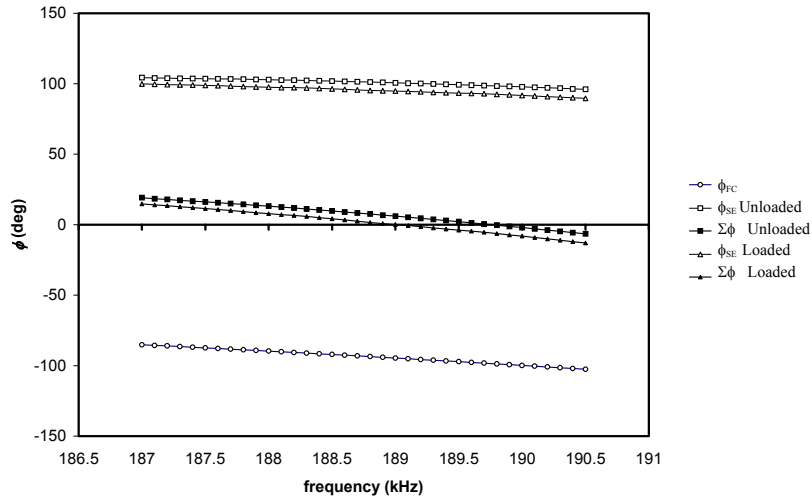


**Figure 10.** Example showing the relationship between resonance frequency of the sensor system and phase-frequency characteristics of the different components in the oscillating circuit. The two uppermost lines show phase shift over the sensor element,  $\phi_{SE}$ , for an unloaded sensor and a sensor applied with  $F_C=9.94 \pm 0.05$  mN (mean $\pm$ SD,  $n=6$ ) to a silicone sample. Note that phase-frequency curves were close to linear and that the change,  $\Delta\phi_{SE}$ , between loaded and unloaded was approximately constant. The bottom line shows phase shift over the feedback loop,  $\phi_{FC}$ . Included are also calculated curves for the total phase shift around the feedback loop,  $\Sigma\phi = \phi_{SE} + \phi_{FC}$  for the different loads. The sensor system will resonate at the frequency where  $\Sigma\phi = 0$ . The shift of the zero cross frequency due to the load was approximately 700 Hz in this example. (From Paper I with permission.)

The CTS used had a spherically shaped contact surface with radius,  $r_0$ , and was applied to the flat surface of the silicone sample. The relationship between contact area,  $A$ , and penetration is described (RÅDE and WESTERGREN, 1990) by:

$$A = 2\pi r_0 L_p \quad (7)$$

Thus,  $\Delta\phi_{SE}$  should be linearly related to contact area  $A$ :

$$\Delta\phi_{SE} = C \cdot A \quad (8)$$

In Paper I it was also shown that  $\Delta f_S$  depends on the change of phase shift,  $\Delta\phi_{SE}$ , over the resonator sensor element through the condition that the phase shift around the feedback loop must be zero (FLOYD, 1988) (Fig. 10).

The two results displayed in Figure 9 and Figure 10 led to the conclusion that the frequency shift in some manner corresponds to the contact area. The model for this relationship was yet to be determined.

In Paper II the relationship between  $\Delta f_S$  and the phase frequency characteristics was modelled with the aim to measure contact area. From the zero phase shift condition (FLOYD, 1988) the sum of phase shifts should be zero:

$$\phi_{FC}(f) + \phi_{SE}(f) = 0 \quad (9)$$

where  $\phi_{FC}(f)$  and  $\phi_{SE}(f)$  are the phase-frequency characteristics of the feedback circuit and the sensor element, respectively. The zero phase condition states that the sensor will oscillate at the frequency at which equation (9) is satisfied. The results of Figure 9 and Figure 10 indicate that the application of the sensor tip against an object causes a net phase shift,  $\Delta\phi_{SE}$ , from the unloaded condition, which according to equation (8) is dependent on contact area:

$${}^{load}\phi_{SE}(f) = {}^{unload}\phi_{SE}(f) + \Delta\phi_{SE}(A) \quad (10)$$

inserted in equation (9)

$$\phi_{FC}(f) + {}^{unload}\phi_{SE}(f) + \Delta\phi_{SE}(A) = 0 \quad (11)$$

Assume that the derivatives of the phase-frequency characteristic for the sensor element,  $d\phi_{SE}/df$ , and for the feedback circuit,  $d\phi_{FC}/df$ , are approximately constant in the interesting frequency range. Figure 10 indicates that this was valid for the CTS. The phase-frequency characteristics for both sensor element and feedback loop could then be written in the form:

$$\phi(f) = \phi(f_0) + \frac{d\phi}{df} \Delta f_S \quad (12)$$

were  $f_0$  is the resonance frequency of an unloaded sensor. Equation (12) for both sensor element and feedback loop inserted in equation (11) gives:

$$\phi_{FC}(f_0) + \frac{d\phi_{FC}}{df} \Delta f_S + \phi_{SE}(f_0) + \frac{d\phi_{SE}}{df} \Delta f_S + \Delta\phi_{SE}(A) = 0 \quad (13)$$

Using equation (9) for the unloaded frequency, that is  $\phi_{FC}(f_0) + \phi_{SE}(f_0) = 0$ , and rearranging the expression yields:

$$\Delta f_S = - \frac{\Delta\phi_{SE}(A)}{\frac{d\phi_{FC}}{df} + \frac{d\phi_{SE}}{df}} \quad (14)$$

This was the model used in Paper II to explain the linear relationship between  $\Delta f_S$  and  $\Delta\phi_{SE}$ . Together with the earlier indication, from Paper I, that  $\Delta\phi_{SE}$  was linearly related to contact area between sensor and measured object, equation (8), it was proposed (Paper II) that  $\Delta f_S$  of the resonator sensor system could be used to estimate contact area and that the relationship should be linear. The high degree of explanation for individual eyes ( $R^2 \geq 0.95$   $n=60$ , Table 1) for an intraocular pressure model based on these assumptions further strengthened the hypothesis that the resonator sensor can be used as a sensitive contact area device with an approximately linear relation between area and  $\Delta f_S$ .

In Paper IV frequency versus indentation was again evaluated. In that study a resonator probe with a slightly convex sensor tip was applied against the cornea of pig eyes under continuous recording. It was shown, by analysing the residual from a linear regression (Normality test,  $p > 0.20$ ,  $n=19959$ , Paper IV), that at an indentation interval of 0.19 mm to 0.49 mm the frequency changed linearly with indentation. A geometric derivation indicated that indentation was close to linearly related to contact area and that the corresponding contact area interval was approximately 5.3 mm<sup>2</sup> to 13.7 mm<sup>2</sup>. For smaller areas, fluid on the cornea will cause an initial fluid contact that affects the frequency shift, and for larger areas the cornea will bend and the full area of the tip will be reached.

In conclusion, there was strong evidence to support the idea that within a certain interval, the frequency change of the sensor system is close to linearly related to the change in contact area. This assumption can be used in the design of experimental models. That is:

$$\frac{df_s}{dA} = Const. \quad (15)$$

## **8.2 A hardness measurement device**

As described in the section 4.4 a number of previous studies have indicated that resonator sensors can be used for hardness or stiffness measurement of an object. In this dissertation the CTS was evaluated for hardness measurement in a silicone model and in an *in vitro* prostate tissue model.

### **8.2.1 Silicone model**

In Paper I, the CTS with spherical contact surface was applied to silicone samples of 5 different hardnesses. The variation in hardness was created by using different mixing ratios of the two components when vulcanising the silicone samples. The hardness of the samples was quoted in the form of penetration values, (mm/10) (DIN ISO 2137, 150g hollow cone. A specified cone is applied to the object with a standardised force and the penetration value after a certain time is recorded. Decreasing penetration values correspond to increasing hardness.). Constant force application of the sensor showed that  $\Delta f_s$  correlated well with the cone penetration standard (Fig. 11) (Paper I). This can be explained through Figure 9 which showed that  $\Delta\phi_{SE}$  was linearly related to penetration depth and equation (14) that linearly transfers the  $\Delta\phi_{SE}$  to the measured frequency shift  $\Delta f_s$ .

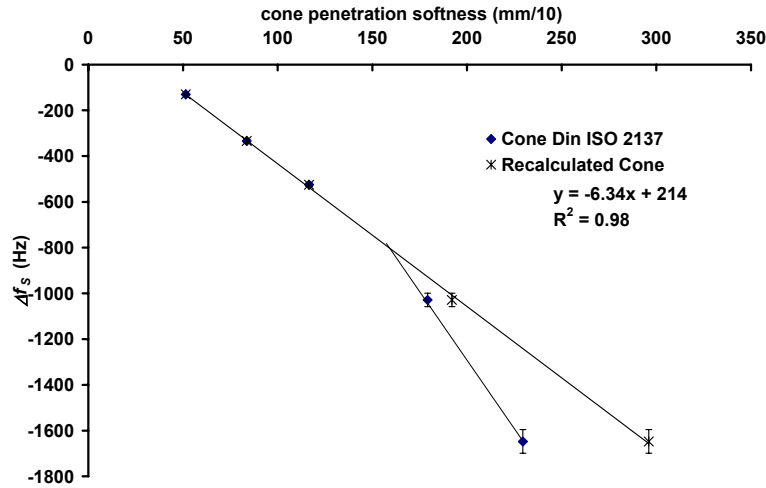


**Figure 11.** Results from Paper I (with permission). Frequency shift of the CTS,  $\Delta f_s$  (mean $\pm$ SEM,  $n=10$ ), vs. cone penetration (DIN ISO 2137) for the five different silicone mixtures.  $\Delta f_s$  is also plotted with regression line versus recalculated cone penetration values. Contact force was  $9.84\pm 0.10$  mN (mean $\pm$ SD,  $n=50$ ). Description of recalculated cone values is given in Paper I.

Therefore, similar to the way of measurement of the penetration depth with the hollow cone in the DIN standard, the penetration depth,  $L_p$ , of the sensor tip into the silicone was measured as a frequency shift of the sensor system. This explained the sensor's capability to measure object hardness under constant force application. The finding that the sensor system could reproducibly differentiate hardness variations between silicone samples of different mixtures was in accordance with earlier reports (LINDAHL and OMATA, 1995). The silicone experiments of Paper I further strengthened the hypothesis that  $\Delta f_s$  measures hardness, and it opens the possibility of referencing the measurement to a known and adopted standard. More importantly, however, was that it explained the physical relationship between  $\Delta f_s$  and hardness of a the measured object.

### 8.2.2 Prostate model

Malignant tumours are generally harder than the surrounding tissue, and this is the reason why tumours often can be detected by palpation. In a recent study a tactile sensor was used to show that the stiffness of resected lymph nodes is an accurate approach to diagnosing lymph node metastases (MIYAJI et al., 1997). In Paper I the CTS was evaluated in an *in vitro* human prostate model. The measurements with constant-force application of the tactile sensor onto the surface of a prostate slice, from a patient suffering from benign

prostate hyperplasia, showed that there were large variations in the frequency shift between measurement sites and small differences within sites (Paper I) (Fig. 12). Experience from the silicon model study (Paper I) indicates, that the differences between sites could be related to differences in hardness. A morphometric analysis of the measurement sites showed that the prostate tissue was mainly composed of prostate gland tissue, stroma and prostate stones. It was assumed that the relative mixture of tissue components would be related to the hardness. An equation (equation (16)) describing the hardness of the prostate tissue based on the relative amounts of glandular tissue ( $Gland_{\%}$ ) and prostate stones ( $Stone_{\%}$ ) was proposed and used:

$$TissuMix = Gland_{\%} + D \cdot Stone_{\%} \quad (16)$$

The best correlation between  $\Delta f_s$  and the tissue mix values was found with  $D=-34$  ( $r=-0.96$ ,  $p<0.001$ ,  $n=60$ ) (Fig. 12).

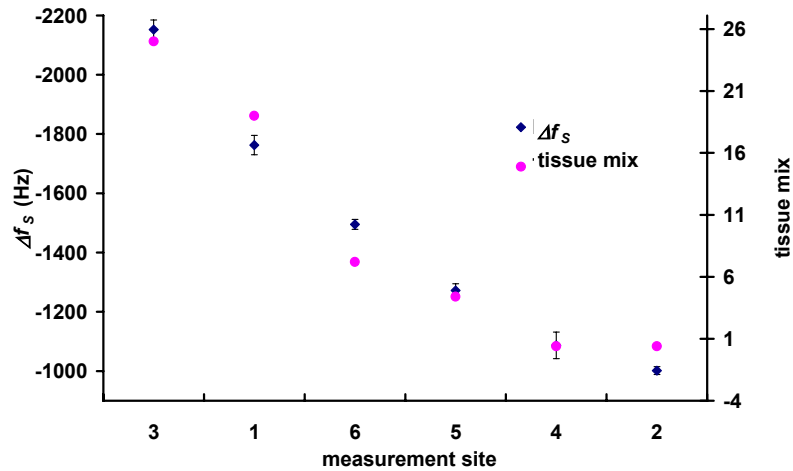


**Figure 12.** Frequency shift,  $\Delta f_s$  (mean $\pm$ SEM,  $n=10$ ), of the CTS applied with constant force,  $F_C=87.6\pm 1.0$  mN (mean $\pm$ SD,  $n=60$ ), vary among the six different measurement sites on a prostate slice. Low SEM indicates that the results were reproducible. TissueMix according to histological investigation and equation (16) are represented by dots. Softer tissue results in a greater negative frequency shift. (From Paper I with permission.)

The study (Paper I) contributed to the work on human tissue hardness since the *in vitro* prostate results indicated that the relative hardness,

interpreted from  $\Delta f_s$ , was correlated to the morphometrically proposed relative tissue hardness. This finding is promising for a further development of a non-invasive tactile sensor for detecting prostate cancer. In the clinical situation it is important for a measurable quantity to have a well-defined, sensor-independent and easily interpreted unit. The DIN ISO 2137 standard used in Paper I might be suitable for defining hardness of human tissue.

### **8.3 An intraocular pressure measurement system**

The applanation principle for intraocular pressure measurement demands knowledge of the contact force and the applanated area. Current methods use some form of constant area and measurement of the force exerted on that area. The resonator sensor evaluated in Paper I was shown to have a frequency shift,  $\Delta f_s$ , that was related to the contact area between the sensor tip and the object it was applied to. This led to the idea to use the contact area measurement capability of the resonator sensor in a new applanation method for IOP measurement.

In Paper II a new sensor for IOP measurement based on the resonator sensor technique was developed and evaluated. It was named it Applanation Resonator Sensor (ARS). The sensor had a contact piece of nylon with a flat surface against the cornea (Fig. 6, left). Enucleated eyes from pigs were pressurised with a saline column connected to the vitreous chamber through a cannula (Fig. 7). The frequency shift (area) of the sensor, applied with constant force against the cornea, was compared with the IOP according to the height of the saline column (Fig. 13).

A model, equation (17), derived from the Imbert-Fick law and the assumption that  $\Delta f_s$  is proportional to the contact area, and that contact force was constant, was fitted against the data.

$$\Delta f_s = \frac{C_{ARS}}{IOP} + C_{Offset} \quad (17)$$

For individual eyes the model showed a high degree of explanation, but for all eyes together  $R^2$  was reduced (Table 1).

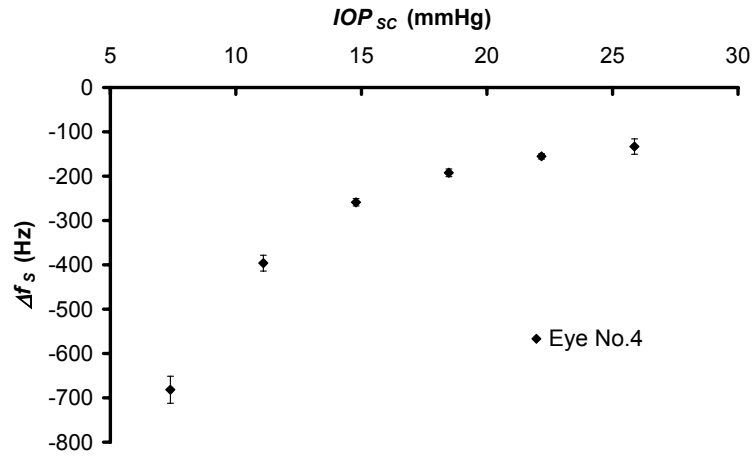


**Figure 13.** Frequency shift ( $\Delta f_s$ , mean,  $n=10$ ) for a flat-surfaced ARS applied to pig-eye cornea with constant force ( $F_c=87.6$  mN) vs. manometric pressure according to saline column. Error bars represent the standard deviation. Measurements taken from a typical eye. (From Paper II with permission.)

**Table 1.** Estimated coefficients,  $C_{ARS}$  and  $C_{Offset}$ , and degree of explanation,  $R^2$ , from the fitting of the model according to equation (17) to the  $\Delta f_s$  and  $IOP_{SC}$  data. Data from Paper II.

Eye No.	$C_{Offset}$	$C_{ARS}$	$R^2$	$n$
Eye 1	127	-5912	0.95	60
Eye 2	123	-5807	0.97	60
Eye 3	168	-6488	0.97	60
Eye 4	111	-5750	0.99	60
Eye 5	31	-4260	0.98	60
Eye 6	-1	-5378	0.97	60
All six eyes	93	-5599	0.92	360

The estimated coefficients for the data from all six eyes (last row Table 1) were used to calculate  $IOP_{ARS}$  from the  $\Delta f_s$  measurement. The overall correlation between  $IOP_{ARS}$ , measured with constant force application, and pressure elicited with the saline column,  $IOP_{SC}$ , was  $r=0.92$  ( $n=360$ , Paper II). The standard deviation for the differences between pairs was 2.6 mm Hg ( $n=360$ , Paper II).

In summary, the study presented in Paper II showed that the resonator sensor principle could be used to measure intraocular pressure in an in vitro

pig-eye model. The sensor technique seem to be suitable for measurement of corneal contact area, and a new IOP measurement application based on the applanation principle was possible. Properties such as good stability, high precision within individual eyes, fast and distinct response of  $\Delta f_s$ , and the possibility of a low contact force were all factors which were promising for the future development. Another important conclusion was that the *in vitro* pig-eye model with the saline column connected to the vitreous chamber could successfully be used to induce variations in IOP (Paper II).

At that stage the main challenges were the differences between eyes and the low resolution at high pressure, when the contact area becomes very small.

In Paper III the same sensor as in Paper II was first evaluated in a clinical study with 24 healthy volunteers. The sensor was applied to the cornea with constant force and  $\Delta f_s$  were recorded. GAT was used as reference method. A significant correlation between  $\Delta f_s$  and  $1/IOP_{GAT}$  ( $r=-0.40$ ,  $p<0.001$ ,  $n=72$ , Paper III) was found. However, the high correlation of the *in vitro* study (Paper II) was not reproduced. There was an unexpectedly large variation in the  $\Delta f_s$  of the ARS sensor when compared with subjects with the same IOP according to GAT. One large difference between the laboratory *in vitro* experimental set-up and the experimental set-up in the clinical situation was the ability to apply the sensor so that the centre of the cornea coincided with the centre of the sensor element contact surface. In the laboratory this can be done very carefully while in the clinical setting the operator has to control this manually. Therefore, the hypothesis that sensitivity to off-centre positioning might be a major source of error was stated (Paper III).

In the same paper (Paper III), the flat probe sensitivity to off-centre positioning was subsequently investigated with the pig-eye model. It showed that even a small off-centre variation of 1 mm could induce variations in  $\Delta f_s$  comparable to the variations found in the clinical evaluation. In an attempt to reduce this sensitivity, a probe with a spherical tip (radius=2.3 mm) was developed. The hypothesis was that for a small off-centre positioning, the convexity of the contact surface would, in comparison with the flat probe, move the centre of contact surface on the sensor closer to the principal axis of the sensor element. The results from an *in vitro* evaluation of the spherical probe showed that the variation due to off-centre positioning was reduced substantially. With positioning within the 1-mm radius around the principal axis the variation of  $\Delta f_s$  was within 11% for the spherical probe as compared with 89% for the flat probe (Paper III). In an evaluation with variation of IOP, the results of the spherical probe showed a high degree of explanation of the

model stated in equation (17) for the individual eyes ( $R^2 \geq 0.97$ ,  $p < 0.001$ ,  $n = 18$ , Paper III), but a reduction of  $R^2$  for all eyes together ( $R^2 = 0.78$ ,  $n = 108$ ,  $p < 0.001$ , Paper III). This was in accordance with the results from Paper II and indicated that there was still an inter-eye variation. A normalisation procedure of  $\Delta f_s$  on each eye reduced the inter-eye differences. With the normalised data, the degree of explanation for the model was  $R^2 = 0.98$  ( $p < 0.001$ ,  $n = 108$ , Paper III). Therefore, further development towards a method and/or signal analysis that incorporates a self-calibration like the normalisation was suggested (Paper III).

A convex tip will diverge from the Imbert-Fick law, which demands a flat contact surface. Instead, the spherical probe method is more comparable to an indentation tonometer, in which a rod is applied to the cornea and the indentation depth is measured (FRIEDENWALD, 1937). For the ARS with the spherical probe the indentation is related to contact area measured through  $\Delta f_s$ . The indentation of the cornea will produce a larger displacement of fluid (MOSES, 1958), a higher increase in IOP (related to the scleral rigidity) and require a larger contact force. The contact force needed was three times greater for the spherical probe than for the flat probe in order to reach the same resolution. It was therefore suggested (Paper III) that, even though the off-centre positioning results of the study (Paper III) supported a strongly convex contact surface, a larger radius of curvature should be considered in order to reduce the penetration, and thereby reduce the needed contact force.

The Imbert-Fick law assumes that the cornea is infinitely thin, perfectly elastic, perfectly flexible and that the only force acting against it is the pressure of the applanated surface (WHITACRE and STEIN, 1993). None of these assumptions are true (WHITACRE and STEIN, 1993). The cornea is not a membrane without thickness and it offers resistance to indentation, varying with its curvature and thickness and the presence or absence of corneal oedema. The surface of the cornea is covered with a liquid film. During the applanation of the cornea, a liquid ring is formed around the contact piece. This will cause capillary attraction or repulsion force between the contact piece and the cornea which will interfere with the measurement (GOLDMANN, 1957). The force term depends on the width of the ring, i.e., the amount of fluid. In addition, the indentation during applanation will rise the IOP, varying with displaced volume and the scleral rigidity of the eye (FRIEDENWALD, 1937).

GOLDMANN (1957) incorporated these forces into an equation governing applanation tonometry:

$$IOP + M' = \frac{F_c}{A} - N' \quad (18)$$

where  $M'$  is the modulus of elasticity of corneal deformation and  $N'$  is the attractive force between the tonometer tip and the cornea. Empirical data of GOLDMANN (1957) indicated that  $M'$  and  $N'$  cancelled out, reducing the equation to the Imbert-Fick law, when the contact diameter was between 2.5 mm and 3.5 mm and optimally with a diameter of 3 mm. Other studies have shown that the Imbert-Fick law is valid for an applanating diameter of 2.8 mm and another study that diameters of 3.53 mm and 3.06 mm produced equally acceptable results (WHITACRE and STEIN, 1993). It seems that there is a contact diameter interval within which the Imbert-Fick law is shown to be a good approximation. However, there are forces not related to IOP that are present, and the magnitude of these forces are dependent on properties such as corneal geometry, amount of tear fluid and disease. These properties will change from eye to eye and even from measurement to measurement. Therefore, measurement methods less dependent on the assumption that the forces cancel out should have a potential to reduce the error in IOP measurement with applanation methods. In Figure 14 a suggestion on how a method using combined continuous measurement of contact area and contact force during an applanation interval, and differential analysis of their relationship is independent of offset forces in that interval.

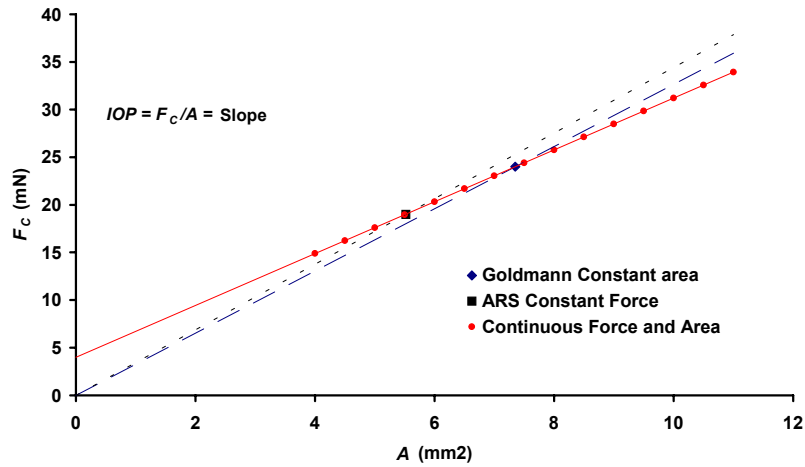


**Figure 14.** Theoretical example of the difference between a one-point method and a multi-point method for determining IOP. An hypothetical constant force of 4 mN, not related to the IOP, is assumed to be measured in the applanation. IOP according to the Imbert-Fick law is interpreted as the slope of the curves. Both methods using one-point readings of force and contact area, Goldmann and ARS with constant force, assume intersection at origin and will overestimate the pressure. A method with combined continuous force and area measurement will be independent of constant forces since the slope is based on the differential change of area and force.

In Paper IV, this new applanation method for IOP measurement which used combined continuous force and area measurement was implemented. Continuous contact area was measured with a resonator sensor device and contact force was measured with a force transducer, both mounted together in one probe. The new ARS was evaluated in our established (Papers II and III) *in vitro* pig-eye set-up. The analysis focused on the initial phase of applanation when the area and force were increasing (Fig.15).

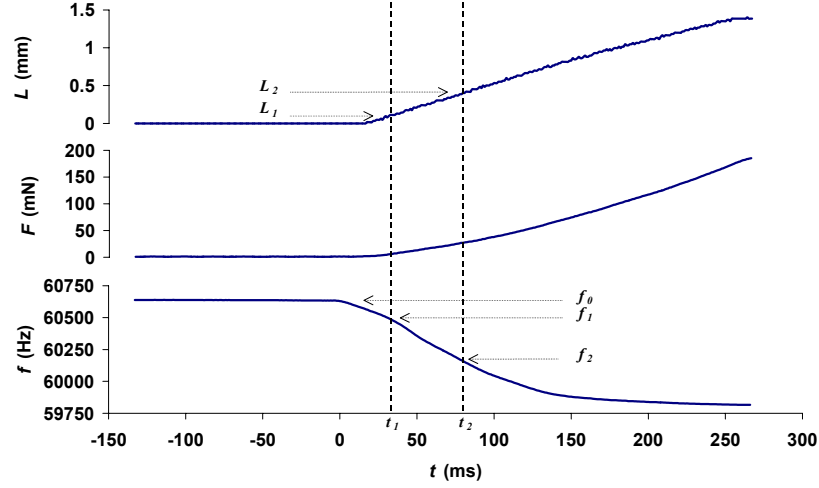


**Figure 15.** Typical measurement taken from the IOP=20 mm Hg level with indentation,  $L$ , force,  $F_C$ , and frequency,  $f$ , as a function of time. It was the initial appplanation phase that was used in the analysis for estimating the pressure. The chosen interval is shown with vertical dotted lines placed at the  $f_1=(f_0 - 150)$  and  $f_2=(f_0 - 470)$  frequencies (Paper IV).

The resonator sensor property of linear relationship between frequency change and area change along with the Imbert-Fick law led to a proposed model with IOP linearly related to the differential relationship between force and frequency:

$$IOP = \beta_1 \frac{dF_C}{df} + \beta_0 \quad (19)$$

$\beta_1$  and  $\beta_0$  are general coefficients. Using the measured pressure in the vitreous chamber,  $IOP_{VC}$ , as reference, the model was fitted against data from six eyes and showed a high degree of explanation ( $R^2=0.989$ ,  $n=414$ , 6 eyes, Fig. 16, Paper IV).

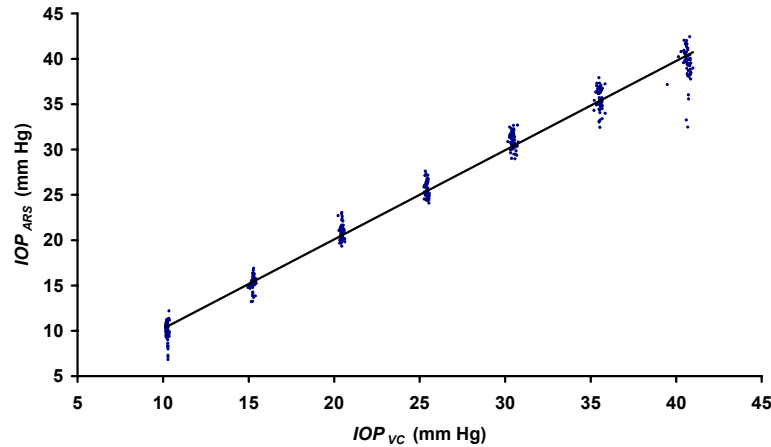


**Figure 16.**  $IOP_{ARS}$  from the applanation resonator method plotted against  $IOP_{VC}$  ( $n=418$ ). To get close to normally distributed residuals, four measurements at the 40 mm Hg level, included in this plot, were regarded as outliers in the evaluation of the model (Paper IV).

This corresponds to a correlation of  $r=0.994$  ( $n=414$ , Paper IV) between  $IOP_{VC}$  and  $IOP_{ARS}$ . A comparison with  $r=0.92$  ( $n=360$ , 6 eyes, Paper II) for the ARS constant force model in Paper II shows that the inter-eye variation was much less with the new method. The overall standard deviation of the residuals from the fit was 1.07 mm Hg ( $n=414$ , Paper IV) indicating that the 95% confidence interval between the  $IOP_{ARS}$  and  $IOP_{VC}$  was  $\pm 2.1$  mm Hg ( $n=414$ , Paper IV). This is in parity with results from Schmidt (SCHMIDT, 1957) for GAT on 4 fresh enucleated human eyes (Residual SD=0.85 mm Hg,  $n=20$ , calculated from Table II) (SCHMIDT, 1957). In addition, the problem with asymptotic behaviour at higher pressure, and corresponding loss of accuracy, associated with the constant force method in Paper II and Paper III, was effectively reduced with the new ARS method that showed an approximately similar accuracy at all pressure levels (Paper IV).

Dependency on off-centre alignment between sensor and cornea was also evaluated in Paper IV. The results showed that a 1 mm off-center alignment could result in a 4 mm Hg overestimation of the  $IOP_{ARS}$  at the 20 mm Hg level (Paper IV). This has to be taken into consideration in the future development of the ARS system.

As described by Friedenwald (FRIEDENWALD, 1937), volume displacement during indentation/applanation will cause a rise in IOP and the magnitude is dependent on the scleral rigidity of the eye. For indentation methods like

Schiötz, a relatively large volume will be displaced resulting in a pressure increase during measurement (MOSES, 1958). With the GAT, the standard contact area guarantees that the displaced volume is small and the pressure in the eye will be elevated only slightly (MOSES, 1958). For handheld indentation-applanation methods with constant area and guard ring such as Tono-Pen, there is no control of the indentation and volume displacement since the operator controls the indentation manually. The area measurement of the ARS method, and choice of area interval for analysis based on that measurement, ensured that the indentation, like the Goldmann method, was small. Thus, the scleral rigidity-related IOP-increase during measurement was controlled and should be approximately the same for all measurements

In summary, Paper IV presented a new methodology for measuring intraocular pressure, to our knowledge never described before. Previous tonometry methods allow one or a few readings of force with constant area for estimating the IOP. The ARS method is the first to combine continuous sampling of both parameters during the application of the sensor onto the cornea, resulting in a linear curve for the force and area relationship. The IOP is then deduced from the slope of that curve, which is based on many points and independent of constant forces. The ARS was evaluated in an *in vitro* pig-eye model and showed good accuracy, good reproducibility with a short measurement time. Consequently, there is a potential for reducing errors in the clinical routine with the use of a device based on this method.

### **8.3.1 Future development**

As described above, the multi-point technique of the new ARS is unique. A comparison with other methods regarding errors due to constant forces associated with the applanation, and a determination of the full value of the method is yet to be performed. However, the distinct improvement from the constant force ARS method is very promising. Already today the accuracy of the ARS in the pig-eye evaluation is in parity with results from Schmidt (SCHMIDT, 1957) for GAT on 4 fresh enucleated human eyes.

There are two problems that must be solved before the ARS can become an instrument for clinical practice. First, the off-centre sensitivity must be further reduced. Secondly, the question regarding sterility procedure must be addressed. The solutions of both of these problems should be feasible.

A study by Rosa et al. (ROSA et al., 1998) showed that GAT measurement after myopic photorefractive keratectomy (PRK) underestimated IOP (mean underestimate > 5 mm Hg,  $n=87$ ) due to thinning of cornea and change in corneal curvature. They identified a risk that PRK patients developing

glaucoma would not be detected in time due to underestimation of IOP. The already convex surface of the ARS contact surface should make it less sensitive to changes in corneal curvature, and it is therefore possible that PRK patients would get a more accurate measurement with that method than with a flat-surfaced method.

Paper IV showed that, for the crucial phase used in the analysis, the continuous ARS only needed approximately 80 ms of contact with the cornea. Therefore, clinical application without requirement of anesthetic may be possible (TOGAWA et al., 1997). In addition, the sensor probe with a combined resonator sensor and force sensor is very compact and easy to apply into a handheld instrument. Since both parameters of the applanation principle are measured and therefore managed by the instrument, no operator adjustments or subjective estimates are needed. A user-friendly tonometer where the operator simply has to touch the cornea with the sensor tip is therefore a reasonable goal for the future research and development.



## 9 General summary and conclusions

The work of this dissertation has further developed and evaluated a resonator sensor technique first presented by Sadao Omata.

For the evaluation an experimental set-up for a silicone model, an *in vitro* prostate tissue model and an *in vitro* pig-eye model was developed.

It was shown in the silicone model study that the hardness according to a catheter tactile resonator sensor (CTS) could be compared to an international cone penetration standard (DIN ISO 2137) (Paper I). A first step towards a non-invasive hardness measurement method for prostate tissue was taken by showing that morphometrically determined tissue composition in a human prostate correlated with the frequency shift of CTS in an *in vitro* study (Paper I).

It was shown in the silicone model (Paper I), and in the *in vitro* pig-eye model (Papers II and IV), that the frequency changes of resonator sensor systems was related to the change in contact area between sensor and silicone, and between sensor and cornea, respectively. In Paper IV it was shown that this relationship was linear over a certain frequency change interval.

The contact area measurement technique was utilised in the development of the applanation resonator sensor (ARS) for measurement of intraocular pressure (IOP). The developed pig-eye model used enucleated pig eyes firmly mounted with agar. For pressurisation a saline column was connected to the vitreous chamber. It was shown that this model could be successfully used to induce variations in IOP for the purpose of evaluating IOP-tonometers (Papers II, III and IV).

A constant force application with a flat-surfaced ARS probe, evaluated in the *in vitro* pig-eye model, showed that contact area measured with the ARS could be used for IOP measurement with good reproducibility and good accuracy within eyes (Paper II). However, a clinical evaluation of the constant force ARS method on healthy human eyes, revealed off-centre alignment between sensor and cornea as a non-negligible source of error and that further development was needed (Paper III).

*In vitro* evaluation of a new probe with a convex contact surface was shown to reduce the off-centre sensitivity. It also indicated that a method incorporating a frequency shift normalisation procedure had the potential to

reduce the between eye differences (Paper III). For that purpose a new ARS method for IOP measurement, using continuous force and area recording during the initial applanating phase, was developed and evaluated in the *in vitro* model. It showed good accuracy, good reproducibility with a short measurement time, and that the between-eye differences were reduced (Paper IV).

The results of this dissertation indicate that a new tonometer, using ARS-technique and continuous force and area recording during the initial applanating phase, is practically possible. The methodology and the sensor technique is new and therefore it has potential to simplify and reduce errors in the clinical routine.

The continuous area measurement capability of the resonator sensor system, disclosed in this dissertation, is unique and there are many possible future applications in medicine and engineering.

## 10 References

- AARNINK, R. G., BEERLAGE, H. P., DE LA ROSETTE, J. J. M. C. H., DEBRUYNE, F. M. J. and WIJKSTRA, H. (1998): 'Transrectal ultrasound of the prostate: Innovations and future applications', *J Urol*, **159**, pp. 1568-1579.
- CANTOR, L. (2000): 'Glaucoma' (The foundation of the American Academy of Ophthalmology, San Fransisco, USA)
- DOUGHTY, M. J. and ZAMAN, M. L. (2000): 'Human corneal thickness and its impact on intraocular pressure measures: a review and meta-analysis approach', *Surv Ophthalmol*, **44**, pp. 367-408.
- EHLERS, N., BRAHMSSEN, T. and SPERLING, S. (1975): 'Applanation tonometry and central corneal thickness', *Acta Ophthalmologica*, **53**, pp. 34-43.
- EISENBERG, D. L., SHERMAN, B. G., MCKEOWN, C. A. and SCHUMAN, J. S. (1998): 'Tonometry in adults and children. A manometric evaluation of pneumatonometry, applanation, and TonoPen in vitro and in vivo', *Ophthalmology*, **105**, pp. 1173-1181.
- FICK, R. (1888): 'Ein neues ophthalmotonometer.', *Pflygers Arch Ges Physiol*, **42**, pp. 159-190.
- FLOYD, T. L. (1988): 'Electronic Devices' (Merrill Publishing Company, Columbus, Ohio)
- FORBES, M., PICO, G. and GROLMAN, B. (1974): 'A noncontact applanation tonometer. Description and clinical evaluation.', *Arch Ophthalmol*, **91**, pp. 134-140.
- FRIEDENWALD, J. S. (1937): 'Contribution to the theory and practice of tonometry', *Am J Ophthalmol*, **20**, pp. 985-1024.
- GOLDMANN, H. (1957): 'Applanation tonometry' *Glucoma. Transactions of the second conference.* (Ed, Newell, F. W.) Josiah Macy, Jr. Foundation,, pp. 167-220.
- GUYTON, A. C. (1991): 'Textbook of Medical Physiology' (Saunders, Philadeplphia)

- HANSEN, M. K. (1995): 'Clinical comparison of the XPERT non-contact tonometer and the conventional Goldmann applanation tonometer.', *Acta Ophthalmol Scand*, **73**, pp. 176-180.
- HODGE, K. K., MCNEAL, J. E., TERRIS, M. K. and STAMEY, T. A. (1989): 'Random systematic versus directed ultrasound guided transrectal core biopsies of the prostate.', *J Urol*, **142**, pp. 71-74; discussion 74-75.
- IKEDA, T. (1990): 'Fundamentals of Piezoelectricity' (Oxford University Press, Oxford)
- IMBERT, A. (1885): 'Théorie des ophthalmotonomètres', *Arch Ophthalmol*, **5**, pp. 358-363.
- JORDAN, G. R. (1985): 'Sensor technologies of the future', *Journal of Physics E (Scientific Instruments)*, **18**, pp. 729-735.
- LANGDON, R. M. (1980): 'Vibratory process control transducers', *Marconi Review*, **43**, pp. 156-175.
- LANGDON, R. M. (1985): 'Resonator sensors-a review', *Journal of Physics E (Scientific Instruments)*, **18**, pp. 103-115.
- LEYDHECKER, W., AKIYAMA, K. and NEUMANN, H. G. (1958): 'Der intraokulare Druck gesunder menschlicher Augen', *Klin Monatsbl Augenheilkd*, **133**, pp. 662-670.
- LINDAHL, O. A. and OMATA, S. (1995): 'Impression technique for the assessment of oedema: comparison with a new tactile sensor that measures physical properties of tissue', *Med Biol Eng Comput*, **33**, pp. 27-32.
- LINDAHL, O. A., OMATA, S. and ANGQUIST, K. A. (1998): 'A tactile sensor for detection of physical properties of human skin in vivo', *J Med Eng Technol*, **22**, pp. 147-153.
- LINDÉN, C. (1997): 'Aspects on Prostanoid and Cholinergic Effects on Aqueous Humour Dynamics in Human Eyes' *Department of Ophthalmology Doctoral Dissertation No 519*, Umeå University, Umeå.
- MACKAY, R. S. and MARG, E. (1959): 'Fast, automatic, electronic tonometers based on an exact theory', *Acta Ophthalmol (Copenh)*, **37**, pp. 495-507.

- MAKLAKOFF, C. (1885): 'L'ophthalmotonometrie', *Arch Ophthalmol*, **5**, pp. 159-165.
- MIDELFART, A. and WIGERS, A. (1994): 'Clinical comparison of the ProTon and Tono-Pen tonometers with the Goldmann applanation tonometer', *Br J Ophthalmol*, **78**, pp. 895-898.
- MINCKLER, D. S., BAERVELDT, G., HEUER, D. K., QUILLEN\_THOMAS, B., WALONKER, A. F. and WEINER, J. (1987): 'Clinical evaluation of the Oculab Tono-Pen.', *Am J Ophthalmol*, **104**, pp. 168-173.
- MIYAJI, K., FURUSE, A., NAKAJIMA, J., KOHNO, T., OHTSUKA, T., YAGYU, K., OKA, T. and OMATA, S. (1997): 'The stiffness of lymph nodes containing lung carcinoma metastases: a new diagnostic parameter measured by a tactile sensor', *Cancer*, **80**, pp. 1920-1925.
- MOORE, K. L. (1992): 'Clinically Oriented Anatomy' (Williams & Wilkins, Baltimore)
- MOSES, R. A. (1958): 'The Goldmann applanation tonometer', *Am J Ophthalmol*, **46**, pp. 865-869.
- MOSES, R. A. and GRODZKI, W. J. J. (1979): 'The pneumatonograph. A laboratory study', *Arch Ophthalmol*, **97**, pp. 547-552.
- OHTSUKA, T., FURUSE, A., KOHNO, T., NAKAJIMA, J., YAGYU, K. and OMATA, S. (1995): 'Application of a new tactile sensor to thoracoscopic surgery: experimental and clinical study.', *Ann Thorac Surg*, **60**, pp. 610-613; discussion 614.
- OMATA, S. (1989): 'Development of new tactile sensor for detecting hardness' *Tech Diagest 8:th Sensor Symp Japan*, pp. 267-270.
- OMATA, S. and CONSTANTINOU, C. E. (1995): 'Modeling of micturition characteristics based on prostatic stiffness modulation induced using hormones and adrenergic antagonists', *IEEE Trans Biomed Eng*, **42**, pp. 843-848.
- OMATA, S. and TERUNUMA, Y. (1991): 'Measurement of skin elasticity using new type tactile sensor and its application to acupuncture therapy' *3rd USA-China-Japan Conference on biomechanics Atalanta, Georgia*, pp. 153-154.
- OMATA, S. and TERUNUMA, Y. (1992): 'New tactile sensor like the human hand and its applications', *Sens. & Actuators*, **35**, pp. 9-15.

- OTTAR, W. L. (1998): 'Tonometry', *Insight*, **23**, pp. 11-17.
- PARKER, V. A., HERRTAGE, J. and SARKIES, N. J. C. (2001): 'Clinical comparison of the Keeler Pulsair 3000 with the Goldmann applanation tonometer', *Br J Ophthalmol*, **85**, pp. 1303-1304.
- QUIGLEY, H. A. and LANGHAM, M. E. (1975): 'Comparative intraocular pressure measurements with the pneumatonograph and Goldmann tonometer.', *Am J Ophthalmol*, **80**, pp. 266-273.
- ROSA, N., CENAMO, G., BREVE, M. A. and LA\_RANA, A. (1998): 'Goldmann applanation tonometry after myopic photorefractive keratectomy.', *Acta Ophthalmol Scand*, **76**, pp. 550-554.
- RÅDE, L. and WESTERGREN, B. (1990): 'Mathematics handbook' (Studentlitteratur, Lund, Sweden)
- SCHMIDT, T. (1957): 'Zur Applanationtonometri an der Spaltlampe', *Ophthalmologica*, **133**, pp. 337-342.
- SOMMER, A. (1989): 'Intraocular pressure and glaucoma.', *Am J Ophthalmol*, **107**, pp. 186-188.
- STEMME, E., EKELOF, J. and NORDIN, L. (1983): 'Measuring liquid density with a tuning-fork transducer', *IEEE Transactions on Instrumentation and Measurement*, **IM-32**, pp. 434-437.
- THORBURN, W. (1978): 'The accuracy of clinical applanation tonometry.', *Acta Ophthalmol (Copenh)*, **56**, pp. 1-5.
- TOBOCMAN, W., RESNICK, M. I. and PRETLOW, T. G. (1997): 'Ultrasound reflections fail to reflect the histopathology of the prostate.', *Prostate*, **30**, pp. 33-40.
- TOGAWA, T., TAMURA, T. and ÖBERG, P. A. (1997): 'Biomedical Transducers and Instruments' (CRC Press, Boca Raton, Florida)
- TORTORA, G. J. and GRABOWSKI, S. R. (1996): 'Principles of Anatomy and Physiology' (Harper Collins Collage Publishers, New York, NY)
- US-DEPT-HHS-PUBL (1993): 'What You Need To Know About Prostate Cancer' #NIH 93-1576 US-Public-Health-Service-National-Institutes-of-Health.
- WAANDERS, J. W. (1991): 'Piezoelectric Ceramics - Properties and Applications' (Philips Components, Eindhoven)

- WATANABE, T., OMATA, S., LEE, J. Z. and CONSTANTINOU, C. E. (1997): 'Comparative analysis of bladder wall compliance based on cystometry and biosensor measurements during the micturition cycle of the rat', *Neurourol Urodyn*, **16**, pp. 567-581.
- WEBER, A. (1867): 'Neues tonometer', *Albrecht von Graefes Arch Ophthalmol*, **13**, pp. 203-209.
- WHITACRE, M. M. and STEIN, R. (1993): 'Sources of error with use of Goldmann-type tonometers', *Surv Ophthalmol*, **38**, pp. 1-30.



## 11 Acknowledgements

I would like to express my sincere thanks to the following:

- Olof Lindahl, my tutor who has become a close friend. You have provided me with excellent guidance in the world of research and in the tricky world outside of science. In spite of your busy schedule you have always had time for me and our research project. Your experience and extensive knowledge in biomedical engineering and your crystal clear values of right and wrong in research have made my work easy and have taught me a lot. We had fun and it was just the start.
- Tomas Bäcklund, your vast knowledge in electronics, mechanics and biomedical engineering, together with your superb practical common sense, have been invaluable for this work. I will remember our discussions, teamwork and comradeship in the lab as one of the best parts of my PhD-student time.
- Stefan Karlsson, for uncompromised support of me and my work, and the whole R&D group at Biomedical Engineering and Informatics, for creating a stimulating, creative, competent and yet very friendly environment for research work. I would especially like to thank: Per Hallberg for his dedicated work with the last stage of the ARS development, my FEM co-workers, Leif Nyström and Daniel Rönnbäck, Urban Wiklund for useful discussions, and Nina Andersson for valuable comments and for enthusiastically keeping the pace on the hydrocephalus research.
- Christina Lindén, co-writer and ophthalmology coach, for believing in my ideas and for inspiring discussions.
- My Japanese friends: with Sadao Omata, who developed the resonator sensor technique, invited me to Koriyama, and taught me its fundamentals; Tim Miller and the rest of the people at Axiom who have all contributed to making this research project very special. The hospitality my family and I met when we visited Japan was fantastic.
- Co-authors, Anders Bergh and Britt Andersson, for fruitful discussions and valuable advice.
- Michael Hansson, for skilful assistance in the clinical study and for useful discussions.

- Waldemar Nyström, for support without pressure.
- Marcus Nääs, for adding new angles into the development work.
- Present head of the Biomedical Engineering and Informatics department, Ronnie Lundström, and former head, Björn-Erik Erlandson, for providing me with resources and support for my research work.
- Jan Malm, although not directly involved in this research project, is worthy of a special thanks; you have been a mentor for me, introduced me to clinical research and continuously given me encouragement.
- NUTEK, VINNOVA, Objective 1 Norra Norrland - EU structural fund, Axiom Co Ltd and BioResonator AB for financial support.
- Britt-Mari Moström, mother-in-law, for your support during the hectic period when I was writing this manuscript.
- Mother and Father for always believing in my ideas and me.
- Finally and most importantly, I wish to thank my family, Maria, Anton and Sanna, for love and support, for putting up with early mornings and late nights, for helping me organize when the tasks were many and the time was limited, and for reminding me that there are other qualities in life than work and research.